NACA

RESEARCH MEMORANDUM

ALTITUDE PERFORMANCE CHARACTERISTICS OF TURBOJET-ENGINE TAIL-PIPE BURNER WITH VARIABLE-AREA EXHAUST NOZZLE USING SEVERAL FUEL SYSTEMS AND FLAME HOLDERS

By LaVern A. Johnson and Carl L. Meyer

Lewis Flight Propulsion Laboratory
Cleveland, Ohio

NATIONAL ADVISORY COMMITTEE
FOR AERONAUTICS

WASHINGTON
December 29, 1950

NATIONAL ADVISORY COMMITTEE FOR AERONAUTICS

RESEARCH MEMORANDUM

ALTITUDE PERFORMANCE CHARACTERISTICS OF TURBOJET-ENGINE TAIL-PIPE BURNER WITH VARIABLE-AREA EXHAUST NOZZLE USING SEVERAL FUEL SYSTEMS AND FLAME HOLDERS

By LaVern A. Johnson and Carl L. Meyer

SUMMARY

A tail-pipe burner equipped with a variable-area exhaust nozzle, which permitted operation over a range of tail-pipe fuel-air ratios at an approximately constant turbine-outlet temperature, has been investigated in the NACA Lewis altitude wind tunnel. Five configurations were investigated over a range of tail-pipe fuel-air ratios at altitudes of 25,000 and 35,000 feet at a flight Mach number of 0.21 to permit selection of a fuel-distribution system and a flame holder for the tail-pipe burner. The best configuration, which included the selected fuel-distribution system and flame holder, was investigated over a range of tail-pipe fuel-air ratios at altitudes from 25,000 to 45,000 feet at a flight Mach number of 0.21, and at flight Mach numbers from 0.21 to 0.83 at an altitude of 25,000 feet.

For the best configuration, an increase in altitude from 25,000 to 45,000 feet at a flight Mach number of 0.21 and a tail-pipe fuel-air ratio of 0.050 lowered the augmented thrust ratio from 1.35 to 1.16, the exhaust-gas total temperature from 3240° to 2480° R, and the tail-pipe combustion efficiency from 0.75 to 0.40, and raised the specific fuel consumption from 2.96 to 3.60. At an exhaust-gas temperature of 3200° R and an altitude of 25,000 feet, an increase in flight Mach number from 0.21 to 0.83 raised the augmented thrust ratio from 1.34 to 1.55, while the specific fuel consumption was constant at approximately 2.93.

INTRODUCTION

An extensive research program on thrust augmentation of turbojet engines is being conducted at the NACA Lewis laboratory. The

performance of several tail-pipe burners with fixed-area exhaust nozzles is reported in references 1 to 4, and the performance of an NACA-designed tail-pipe burner with a variable-area exhaust nozzle is reported in reference 5. As an additional part of this program, the performance of a second tail-pipe burner with a variable-area exhaust nozzle has been investigated in the altitude wind tunnel. The tail-pipe burner was installed on an axial-flow-compressor-type turbojet engine and was supplied by the engine manufacturer as an integral component of this engine.

For this second tail-pipe burner with variable-area exhaust nozzle, performance data obtained at two altitudes with each of five configurations are compared to permit selection of a fuel-distribution system and flame holder. The modifications to the original fuel-distribution system and flame holder were based on the results of references 1 to 4, which indicate the effect of fuel system and flame-holder design on burner performance as well as the effect of altitude and flight Mach number on over-all performance with fixed-area exhaust nozzles. Performance data obtained for the selected tail-pipe-burner configuration over a range of altitudes and flight Mach numbers are presented to show the effect of these variables on over-all performance. The data for each configuration and flight condition are presented for a range of tail-pipe fuel-air ratios at an approximately constant turbine-outlet temperature. All data obtained with each configuration are presented in tabular form. Operational characteristics of the tail-pipe burner are also discussed.

APPARATUS

Engine

The J47 turbojet engine used in this investigation has a static sea-level rating of 5000 pounds thrust at an engine speed of 7900 rpm and a turbine-outlet temperature of 1735° R. The air flow is approximately 94 pounds per second and the fuel consumption is 5250 pounds per hour at this operating condition. The over-all length of the engine including the standard tail pipe is 143 inches, the maximum diameter is 37 inches, and the total weight is 2475 pounds. The length of the standard tail pipe including a fixed-area exhaust nozzle is 55 inches. The main components of the engine include a 12-stage axial-flow compressor, eight cylindrical through-flow combustors, a single-stage turbine, and a tail pipe.

Tail-Pipe-Burner Assembly

The tail-pipe burner assembly used in this investigation was supplied by the engine manufacturer and was intended to be an integral component of the engine. The tail-pipe-burner assembly (fig. 1) has an over-all length of approximately 121 inches with the variable-area exhaust nozzle in the open position. The assembly consists of three sections: (1) a diffuser section $49\frac{7}{8}$ inches long, tapering from an inlet diameter of 35 inches to an outlet diameter of approximately $30\frac{1}{2}$ inches, and having an inlet to outlet area ratio of 0.686; (2) a combustion chamber having an over-all length of $60\frac{7}{8}$ inches, of which the forward $35\frac{1}{8}$ inches is a converging conical section and the aft $25\frac{3}{4}$ inches is a cylindrical section; and (3) a variable-area exhaust nozzle having a length of $10\frac{5}{16}$ inches with the nozzle in the open position.

The downstream end of the diffuser inner body has an internal diameter of $13\frac{3}{8}$ inches, a 1/2-inch external flange, and a concave dome with a depth of $8\frac{1}{2}$ inches to provide a sheltered region for seating a stabilizing flame in the center of the combustion chamber. Flame holders for each configuration were installed 18 inches downstream of the combustion-chamber inlet.

A cooling liner was installed in the combustion chamber $24\frac{3}{8}$ inches downstream of the combustion-chamber inlet and extended to within $1\frac{3}{8}$ inches of the outlet of the fixed portion of the variable-area exhaust nozzle. A radial space of $\frac{9}{16}$ inch was provided between the liner and the burner shell through which a small portion of the tail-pipe gas flowed at approximately turbine-outlet temperature to cool the burner shell.

The variable-area exhaust nozzle (fig. 2) consists of a fixed conical section $10\frac{5}{16}$ inches long and two movable lips so interconnected that the lips move simultaneously over the inner fixed section. The nozzle is so constructed that the outlet area is circular

for both open and closed positions, except that in the open position the four corners of the movable lips protrude into the outlet area. For all intermediate positions the outlet was irregular in shape. The nozzle has a maximum projected discharge area of 452 square inches and a minimum to maximum area ratio of 0.569. A seal made of metal strips was placed between the fixed and movable portions of the nozzle to prevent leakage (fig. 2(a)).

The tail-pipe-burner assembly, as received from the manufacturer, included an ignition system that consisted of a fuel nozzle and two spark plugs mounted in the concave dome at the downstream end of the diffuser inner body. A second system, installed at the Lewis laboratory as an auxiliary system for this investigation, provided ignition by a momentary injection of high-pressure fuel into one of the engine combustors; this excess fuel produced a streak of flame through the turbine to ignite the fuel-air mixture in the tail-pipe burner. Further details of the second system are given in reference 2.

INSTALLATION AND INSTRUMENTATION

The engine and tail-pipe-burner assembly were mounted on a wing section that spanned the 20-foot-diameter test section of the altitude wind tunnel (fig. 3). Dry refrigerated air was supplied to the engine inlet through a duct from the tunnel make-up air system. This duct was connected to the engine by use of a slip joint with a frictionless seal, which made possible the measurement of thrust and drag with the tunnel balance scales. In order to simplify the installation and to provide accessibility for instrumentation, no cowling was installed.

Instrumentation was installed at several stations in the engine as shown in figure 4. The temperature and pressure measurements obtained at the engine inlet (station 1) were used to calculate air flow; instrumentation installed at the turbine outlet (station 6) was used to measure the tail-pipe-burner inlet conditions, and measurements obtained at the exhaust-nozzle outlet (station 8) were used in calculating the exhaust-gas total temperature. Four static wall orifices were installed ahead of the flame holder at station 7 (fig. 1). Fuel flows to the engine and tail-pipe burner were measured by calibrated rotameters.

Description of Configurations

Five configurations were investigated; the original configuration is designated A and the four modified configurations are designated B, C, D, and E. All configurations had fuel-spray bars located at stations A and B (fig. 1); in addition, fuel-spray nozzles were located at station C for configuration A. A flow divider proportioned the fuel between the various stations; the flow divider schedules for the various configurations are shown in figure 5. Station D (fig. 1) is the flame holder location for configurations A, B, C, and D.

Configuration A. - The flame holder (fig. 6) and the fuel system (fig. 7) used in configuration A were supplied by the engine manufacturer. This flame holder was an unsymmetric V-gutter type and had a blocked area of 23 percent of the burner cross-sectional area. Fuel was injected perpendicular to the direction of gas flow through orifices drilled in radial spray bars located at stations A and B and in the direction of gas flow from conical spray nozzles at station C. The schedule of the flow divider installed in the main fuel line was such that at low fuel flows, corresponding to high-altitude operation, fuel from the small port of the flow divider was injected through the fuel bars at station B and through six of the spray nozzles located at station C. For higher tail-pipe fuel flows, additional fuel from the large port of the flow divider was injected through the remaining nozzles at station C and through the fuel bars at station A.

Configuration B. - The same flame holder was used for configuration B as for configuration A; however, the fuel system was modified (fig. 8) to provide a more uniform fuel distribution across the burner section. The conical spray nozzles at station C were omitted and all of the fuel was injected perpendicular to the direction of gas flow from spray bars at stations A and B. All the fuel from the small port side of the flow divider was injected at station B and fuel from the large port side was injected at station A.

Configuration C. - The flame holder used in configurations A and B was also used in configuration C. In order to obtain a still more uniform mixture of fuel and air for configuration C (fig. 9) the fuel bars at station B were replaced by bars having a larger number of discharge holes so located that the fuel would be injected closer to the outer wall of the diffuser section. All fuel from the small port side of the flow divider was injected at station B and fuel from the large port side was injected at station A.

Configuration D. - A double V-gutter type flame holder (fig. 10), which had a blocked area of 31 percent of the burner cross-sectional

area, was installed for configuration D to provide a greater blocking area for seating the flame. The inner flame-holder diameter was considered the minimum that would prevent overheating of the flame holder by the stabilizing flame seated on the diffuser cone. The outer flame-holder diameter was considered the maximum that would prevent overheating the outer shell and cooling liner of the burner. As a result, the two annular rings of the flame holder were fairly close together and the inner ring was therefore placed $2\frac{1}{4}$ inches downstream from the outer ring to prevent excessive flow interference between the two rings and to maintain the velocity over each ring as low as possible. The fuel system used in this configuration was the same as that used with configuration C.

Configuration E. - In order to determine the performance obtainable with a minimum blocking area, only the diffuser cone was used as the flame seat for configuration E. The fuel system used was the same as that of configurations C and D.

The five configurations investigated are summarized in the following table:

Configuration	Flame holder	Projected area of flame holder (percent of burner cross-sectional area)	Fuel system
A	Unsymmetric V-gutter (fig. 6)	23	Original (fig. 7)
B	Unsymmetric V-gutter (fig. 6)	23	First modification (fig. 8)
C	Unsymmetric V-gutter (fig. 6)	23	Second modification (fig. 9)
D	Double V-gutter (fig. 10)	31	Second modification (fig. 9)
E			Second modification (fig. 9)

PROCEDURE

The performance of each configuration was investigated over a range of tail-pipe fuel-air ratios at a flight Mach number of 0.21 at altitudes of 25,000 and 35,000 feet to obtain comparable data which would permit selection of a fuel-distribution system and

flame holder for the tail-pipe burner. The performance of the selected configuration was then investigated over a range of tail-pipe fuel-air ratios at a flight Mach number of 0.21 at altitudes from 25,000 to 45,000 feet and over a range of flight Mach numbers from 0.21 to 0.83 at an altitude of 25,000 feet. In order to simulate these flight conditions, air supplied from the tunnel make-up air system was throttled from approximately sea-level pressure to the desired pressure at the engine inlet, while the tunnel test-section pressure was maintained to simulate the desired altitude.

As the tail-pipe fuel-air ratio was varied at each flight condition, the variable-area exhaust nozzle was adjusted to maintain an approximately constant turbine-outlet temperature of 1710° R (within ±50°). This temperature of 1710° R was selected as the operating temperature instead of the rated temperature of 1735° R to conserve turbine life.

At each flight condition the engine was operated at rated speed and the engine-inlet temperature was maintained at 500° R ±10°. This engine-inlet temperature is higher than the NACA standard temperatures for the flight conditions investigated; the difference is greatest for a flight Mach number of 0.21 at altitudes of 35,000 and 45,000 feet, for which the standard temperatures are approximately equal. Although the general performance level of the tail-pipe burner and engine would have been higher if the standard inlet temperatures had been used, the relative effect of altitude is approximately correct as presented herein. If, for example, the inlet temperature at an altitude of 25,000 feet had been adjusted to maintain the ratio of inlet to standard temperatures that was maintained at altitudes of 35,000 and 45,000 feet, the turbine-outlet total pressure would have been changed only about 2 percent. This change in turbine-outlet pressure is small compared with a reduction in turbine-outlet total pressure of about 40 percent when the altitude was increased from 25,000 to 35,000 feet and would have negligible effect on the data showing the effect of altitude on tail-pipe burner performance.

Fuel conforming to the specification AN-F-32 with a lower heating value of 18,550 Btu per pound and a hydrogen-carbon ratio of 0.155 was used in the engine, and fuel conforming to the specification AN-F-48b, grade 80, unleaded gasoline, with a lower heating value of 19,000 Btu per pound and a hydrogen-carbon ratio of 0.186 was selected for use in the tail-pipe burner.

The methods of calculations and the symbols used are presented in the appendix.

RESULTS AND DISCUSSION

All of the data obtained with each configuration are presented in table I. The combustion-chamber-inlet velocity was of the order of 500 feet per second; this velocity increased 1 to 3 percent for the various configurations as the altitude was raised from 25,000 to 35,000 feet. Data for configuration D indicate that the combustion-chamber-inlet velocity increased 5 to 6 percent as the altitude was raised from 25,000 to 45,000 feet and remained essentially constant as the flight Mach number was raised from 0.21 to 0.83.

Effect of Burner Modifications

Fuel distribution. - The variation of tail-pipe burner performance with tail-pipe fuel-air ratio for configurations A, B, and C is presented in figures 11 and 12 for altitudes of 25,000 and 35,000 feet at a flight Mach number of 0.21. Tail-pipe fuel-air ratio is defined as the weight flow of fuel injected into the tail-pipe burner divided by the weight flow of unburned air entering the tail pipe. The augmented thrust ratio is defined as the ratio of augmented net thrust to the net thrust obtainable with the standard engine tail pipe at rated engine speed. Turbine-outlet total temperatures indicated on the figures show the range of temperature within which data were obtained at each flight condition.

Data for an altitude of 25,000 feet (fig. 11) indicate that, for the uniform fuel distribution of configuration C, the tail-pipe-burner combustion efficiency increased with increasing fuel-air ratio to a maximum value at a fuel-air ratio of approximately 0.055 and then decreased at higher fuel-air ratios. For the less uniform fuel distributions of configurations A and B, however, the tail-pipe-burner combustion efficiency decreased progressively as the fuel-air ratio was increased. Data for an altitude of 35,000 feet (fig. 12), however, do not show the aforementioned trends of combustion efficiency with fuel-distribution uniformity. Configuration C, with which the lowest specific fuel consumption and the highest thrust augmentation, exhaust-gas total temperature, and tail-pipe-burner combustion efficiency were obtained at all fuel-air ratios at an altitude of 35,000 feet and at fuel-air

ratios above approximately 0.045 at an altitude of 25,000 feet, was selected as the best fuel-distribution system investigated. Performance with configuration A was poorer than with the other configurations at both altitudes.

Flame-holder design. - The variation of tail-pipe-burner performance with tail-pipe fuel-air ratio for the flame-holders of configurations C, D, and E is presented in figures 13 and 14 for altitudes of 25,000 and 35,000 feet and a flight Mach number of 0.21. The same fuel system was used for each configuration. The specific fuel consumption was lower and the augmented thrust ratio, exhaust-gas total temperature, and tail-pipe combustion efficiency were higher for configuration D, the double V-gutter flame holder, than with the other two configurations except at the highest fuel-air ratios at an altitude of 25,000 feet when configuration C appeared slightly better. Configuration E, which used only the diffuser cone for a flame seat, gave performance inferior to that of both the other flame-holder configurations, except at tail-pipe fuel-air ratios below approximately 0.043 and an altitude of 25,000 feet when the performance was better than that of configuration C.

Configuration D was considered the best of those investigated because of the improved performance over the others for most of the range of operating conditions investigated. The maximum tail-pipe combustion efficiencies obtained with this configuration were 0.76 at a tail-pipe fuel-air ratio of 0.037 and an altitude of 25,000 feet, and 0.70 at a tail-pipe fuel-air ratio of 0.041 and 35,000 feet.

Over-All Performance

The effect of altitude and flight Mach number on tail-pipe-burner performance for a range of tail-pipe fuel-air ratios with configuration D, which was considered to be the best of those investigated, is presented in figures 15 to 18.

Effect of altitude. - The effect of an increase in altitude from 25,000 to 45,000 feet at a flight Mach number of 0.21 on tail-pipe-burner performance is shown in figure 15. For the range of tail-pipe fuel-air ratios investigated, an increase in altitude lowered the augmented thrust ratio, exhaust-gas total temperature, and tail-pipe combustion efficiency, and raised the specific fuel consumption. At a tail-pipe fuel-air ratio of 0.050, an increase in altitude from 25,000 to 45,000 feet lowered the augmented thrust ratio from 1.35 to 1.16, the exhaust-gas total

temperature from 3240° to 2480° R, and the tail-pipe combustion efficiency from 0.75 to 0.40, and raised the specific fuel consumption from 2.96 to 3.60. This effect of altitude on performance is primarily due to a decrease in combustion-chamber-inlet pressure of about 63 percent as the altitude was raised from 25,000 to 45,000 feet; the combustion-chamber-inlet total temperature was approximately constant and the velocity increased only 5 to 6 percent.

At an altitude of 25,000 feet, the exhaust-gas total temperature and augmented thrust ratio increased continuously with tail-pipe fuel-air ratio up to a fuel-air ratio of 0.050, the maximum for which data were obtained. For altitudes of 35,000 and 45,000 feet, however, the exhaust-gas total temperature tended to level off at a tail-pipe fuel-air ratio of approximately 0.045 and consequently the rate of increase of the augmented thrust ratio decreased at this tail-pipe fuel-air ratio.

Effect of flight Mach number. - The effect of flight Mach number on tail-pipe-burner performance is presented for an altitude of 25,000 feet and flight Mach numbers of 0.21, 0.53, and 0.83 in figure 16. A limited amount of data were available at a flight Mach number of 0.83; therefore, three data points are presented for which the turbine-outlet temperature was slightly below the lower temperature limit. As the flight Mach number was raised from 0.21 to 0.83, the combustion-chamber-inlet pressure increased approximately 52 percent, but the combustion-chamber-inlet velocity and total temperature remained essentially constant. Over the range of tail-pipe fuel-air ratios investigated, an increase in flight Mach number from 0.21 to 0.83 raised the augmented thrust ratio but had no apparent effect on exhaust-gas total temperature, tail-pipe combustion efficiency, or specific fuel consumption. At each flight Mach number, the exhaust-gas total temperature and augmented thrust ratio continued to increase with tail-pipe fuel-air ratio up to a fuel-air ratio of approximately 0.052, the maximum investigated. As the tail-pipe fuel-air ratio was raised from 0.030 to 0.052, the tail-pipe combustion efficiency remained approximately constant, the specific fuel consumption increased from 2.38 to 3.05, and the exhaust-gas total temperature increased from 2710° to 3290° R.

The results presented in figure 16 are cross-plotted in figure 17 to show the variation of performance with flight Mach number for exhaust-gas total temperatures of 3000° and 3200° R. The performance variation with flight Mach number is similar for both exhaust-gas temperatures. For an exhaust-gas temperature of 3200° R, an increase in flight Mach number from 0.21 to 0.83

increased the augmented thrust ratio from 1.34 to 1.55, the specific fuel consumption was constant at approximately 2.93, and the total fuel-air ratio was approximately 0.053. For this increase in flight Mach number, the specific fuel consumption with the standard engine tail pipe increased from 1.27 to 1.40.

Although the augmented thrust ratio did not increase with flight Mach number as rapidly as might be expected, the augmented thrust increased rapidly as shown in figure 18, where the variation in net thrust with flight Mach number is presented for the standard engine tail pipe and for tail-pipe burning. For an increase in flight Mach number from 0.21 to 0.83, the augmented thrust increased about 60 percent and the standard engine thrust increased about 40 percent.

Operational Characteristics

Range of tail-pipe fuel-air ratios. - The minimum and maximum operable tail-pipe fuel-air ratios were not determined for the various configurations. The minimum tail-pipe fuel-air ratio at which performance data were obtained was approximately 0.025; operation at lower fuel-air ratios was not considered of interest. In general, performance data were obtained at progressively higher tail-pipe fuel-air ratios until either the augmented thrust appeared to have reached a maximum or limiting turbine-outlet temperature was obtained with the exhaust nozzle fully open. For configuration D, limiting turbine-outlet temperature was obtained or apparently could have been obtained with the exhaust nozzle fully open at all flight conditions investigated except at an altitude of 45,000 feet; the tail-pipe fuel-air ratio required at these conditions varied from approximately 0.040 to 0.052. With the exhaust nozzle fully open, limiting turbine-outlet temperature could not be obtained for configurations A and E at either of the two flight conditions investigated, and could be obtained for configurations B and C only at an altitude of 25,000 feet at tail-pipe fuel-air ratios of approximately 0.063 and 0.045, respectively.

Ignition systems. - Two ignition systems were available throughout the investigation to provide ignition of the tail-pipe-burner fuel; starting limits were not determined for either system. It is estimated that over 100 starts were made with the ignition system that consisted of a fuel nozzle and two spark plugs mounted in the concave section at the downstream end of the diffuser inner body. Approximately 20 starts were made by means of a flame streak from one of the engine combustors. Both ignition systems were reliable except for infrequent fouling of the spark plugs in the first system; the flame-streak method was then used to avoid shutdown.

Tail-pipe-burner shell cooling. - Tail-pipe-burner shell cooling was provided by the flow of a small portion of the relatively cool turbine-outlet gas through the passage between the cooling liner and the shell; this method apparently provided adequate cooling at all flight conditions investigated except at a flight Mach number of 0.83 at an altitude of 25,000 feet. After an estimated operating time with tail-pipe burning of $11\frac{1}{2}$ hours, however, the cooling liner collapsed. A second liner was installed and it provided adequate cooling without failure for the remaining $3\frac{1}{2}$ hours of tail-pipe-burner operation. Both liners were supported by hat-section stiffeners; other methods of support (reference 5) have been used to provide adequate support against the pressure difference which caused the first liner to collapse.

Warping of the exhaust nozzle, which caused the movable lips to bind and some of the metal strip seals to burn away, was encountered at the higher tail-pipe fuel flows at a flight Mach number of 0.83 at an altitude of 25,000 feet.

CONCLUDING REMARKS

A tail-pipe burner with a variable-area exhaust nozzle, which permitted operation over a range of tail-pipe fuel-air ratios at an approximately constant turbine-outlet temperature, has been investigated in the NACA Lewis altitude wind tunnel. Five configurations were investigated at two altitudes to permit selection of a fuel-distribution system and a flame holder for the tail-pipe burner. The performance of the best configuration, which included the selected fuel-distribution system and flame holder, was determined over a range of altitudes and flight Mach numbers. The following statements pertain to the best configuration:

An increase in altitude from 25,000 to 45,000 feet at a flight Mach number of 0.21 and a tail-pipe fuel-air ratio of 0.050 lowered the augmented thrust ratio from 1.35 to 1.16, the exhaust-gas total temperature from 3240° to 2480° R, and the tail-pipe combustion efficiency from 0.75 to 0.40, and raised the specific fuel consumption from 2.96 to 3.60.

An increase in flight Mach number at a given tail-pipe fuel-air ratio and at an altitude of 25,000 feet resulted in an increase in augmented thrust ratio, but the specific fuel consumption, exhaust-gas total temperature, and tail-pipe combustion efficiency were

unaffected. At an exhaust-gas temperature of 3200° R, an increase in flight Mach number from 0.21 to 0.83 at an altitude of 25,000 feet raised the augmented thrust ratio from 1.34 to 1.55, while the specific fuel consumption was constant at approximately 2.93.

Lewis Flight Propulsion Laboratory,
National Advisory Committee for Aeronautics,
Cleveland, Ohio.

APPENDIX - CALCULATIONS

Symbols

The following symbols are used in this report:

A	cross-sectional area, sq ft
B	thrust-scale reading, lb
C_j	jet thrust coefficient, ratio of scale jet thrust to rake jet thrust
C_T	thermal-expansion ratio, ratio of hot-exhaust-nozzle area to cold-exhaust-nozzle area
D	external drag of installation, lb
D_R	drag of exhaust-nozzle survey rake, lb
F_j	jet thrust, lb
F_n	net thrust, lb
f/a	fuel-air ratio
g	acceleration of gravity, ft/sec^2
H	total enthalpy, Btu/lb
h_c	lower heating value of fuel, Btu/lb
M	Mach number
P	total pressure, lb/sq ft absolute
p	static pressure, lb/sq ft absolute
R	gas constant, 53.4, ft-lb/(lb)($^\circ$R)
T	total temperature, $^\circ$R
T_i	indicated total temperature, $^\circ$R
t	static temperature, $^\circ$R

V	velocity, ft/sec
W_a	air flow, lb/sec
W_c	compressor leakage air flow, lb/sec
W_f	fuel flow, lb/hr
W_f/F_n	specific fuel consumption based on total fuel flow and net thrust, lb/(hr)(lb thrust)
W_g	gas flow, lb/sec
γ	ratio of specific heats for gases
η_b	burner combustion efficiency

Subscripts:

a	air
e	engine
f	fuel
g	gas
j	station where jet static pressure equals ambient static pressure
m	fuel manifold
r	rake
s	scale
t	tail-pipe burner
x	inlet duct at labyrinth slip joint
0	ambient conditions
1	engine inlet
3	compressor outlet (inlet to engine combustors)

6 turbine outlet (tail-pipe diffuser inlet)

7 station $2\frac{1}{8}$ inches upstream of flame holder

8 station 1 inch upstream of fixed portion of nozzle outlet

8' exhaust-nozzle survey station in standard-engine tail-pipe

Methods of Calculation

Flight Mach number and airspeed. - Flight Mach number and equivalent airspeed were calculated by the following equations using engine-inlet total pressure and temperature and assuming complete free-stream total-pressure recovery:

$$M_0 = \sqrt{\frac{2}{\gamma_1 - 1}\left[\left(\frac{P_1}{p_0}\right)^{\frac{\gamma_1 - 1}{\gamma_1}} - 1\right]} \tag{1}$$

$$V_0 = M_0 \sqrt{\gamma_1 g R T_1 \left(\frac{p_0}{P_1}\right)^{\frac{\gamma_1 - 1}{\gamma_1}}} \tag{2}$$

Temperature. - Static temperatures were calculated from indicated temperatures using the following relation:

$$t = \frac{T_i}{1 + 0.85\left[\left(\frac{P}{p}\right)^{\frac{\gamma - 1}{\gamma}} - 1\right]} \tag{3}$$

The type of thermocouple used has an impact recovery factor of 0.85.

Air flow. - Air flow at the engine inlet was calculated from the following equation using the pressure and temperature measurements obtained in the inlet annulus:

$$W_{a,1} = p_1 A_1 \sqrt{\frac{2\gamma_1 g}{(\gamma_1 - 1) R t_1}\left[\left(\frac{P_1}{p_1}\right)^{\frac{\gamma_1 - 1}{\gamma_1}} - 1\right]} \tag{4}$$

The leakage air flow through the labyrinth seal in the compressor was experimentally determined and subtracted from the air flow measured at station 1 to obtain the air flow entering the engine combustors:

$$W_{a,3} = W_{a,1} - W_c \tag{5}$$

Gas flow. - Gas flow at the turbine outlet was determined from the relation:

$$W_{g,6} = W_{a,3} + \frac{W_{f,e}}{3600} \tag{6a}$$

Gas flow through the tail-pipe burner was calculated from the following relation:

$$W_{g,7} = W_{g,8} = W_{a,3} + \frac{W_{f,e} + W_{f,t}}{3600} \tag{6b}$$

Fuel-air ratio. - The tail-pipe burner fuel-air ratio used herein is defined as the weight flow of fuel supplied to the tail-pipe burner divided by the weight flow of unburned air entering the tail-pipe burner. Weight flow of unburned air was determined by assuming that the fuel injected in the engine combustors was completely burned. The tail-pipe fuel-air ratio was obtained by combining engine fuel flow, tail-pipe-burner fuel flow, and air flow in the following relation:

$$(f/a)_t = \frac{W_{f,t}}{3600\ W_{a,3} - \frac{W_{f,e}}{0.068}} \tag{7}$$

where 0.068 is the stoichiometric fuel-air ratio for the engine fuel.

The total fuel-air ratio for the engine and tail-pipe burner is

$$(f/a) = \frac{W_{f,e} + W_{f,t}}{3600\ W_{a,3}} \tag{8}$$

Combustion-chamber-inlet velocity. - Velocity at the tail-pipe-burner combustion-chamber inlet was calculated from the equation of continuity using the static pressure measured at station 7 (fig. 1) and assuming that the total pressure and the total temperature remained constant from the turbine outlet to the combustion-chamber inlet:

$$V_7 = \frac{R\, W_{g,7}\, T_6}{A_7\, p_7} \left(\frac{p_7}{P_6}\right)^{\frac{\gamma_6-1}{\gamma_6}} \tag{9}$$

Augmented thrust. - The augmented jet thrust was determined from balance-scale measurements by using the following equation:

$$F_{j,s} = B + D + D_R + \frac{W_{a,1}\, V_x}{g} + A_x(p_x - p_0) \tag{10}$$

The last two terms in this equation are the momentum and pressure forces acting on the installation at the slip joint in the make-up air duct. The external drag of the installation was determined from power-off drag tests. The exhaust-nozzle survey-rake drag was measured hydraulically.

The augmented net thrust was determined by subtracting the free-stream momentum of the inlet air from the augmented jet thrust:

$$F_n = F_{j,s} - \frac{W_{a,1}\, V_0}{g} \tag{11}$$

Jet-thrust coefficient. - The jet-thrust coefficient C_j is defined as the ratio of scale jet thrust to rake jet thrust.

$$C_j = \frac{F_{j,s}}{F_{j,r}} = \frac{F_{j,s}}{C_T A_8 M_8 M_j \gamma_8 p_8 \left(\frac{p_0}{p_8}\right)^{\frac{\gamma_8-1}{2\gamma_8}}} \tag{12}$$

Mach number M_8 was determined from P_8 and p_8 and M_j was determined from P_8 and p_0. The thermal-expansion ratio C_T was based on exhaust-nozzle skin temperature. Values of C_j calculated from experimental data are shown in figure 19.

Standard engine thrust. - The net thrust for the standard engine was calculated from measurements of turbine-outlet total temperature, total pressure, and gas flow obtained during the tail-pipe-burning investigation, by use of the following relation:

$$F_{n,e} = \frac{W_{g,6}}{g} C_j \sqrt{\frac{2\gamma_6 gRT_{8'}}{\gamma_6 - 1}\left[1 - \left(\frac{p_0}{p_{8'}}\right)^{\frac{\gamma_6 - 1}{\gamma_6}}\right]} - \frac{W_{a,1} V_0}{g} \qquad (13)$$

During calibration of the engine with a standard tail pipe, the total pressure at the exhaust-nozzle outlet was found to be 0.97 of the turbine-outlet total pressure. Accordingly, the value of the total pressure $P_{8'}$ in equation (13) was taken as 0.97 P_6. The temperature $T_{8'}$ was assumed equal to T_6. Values of C_j were obtained from figure 19(a).

Exhaust-gas total temperature. - The exhaust-gas total temperature was calculated from scale jet thrust, exhaust-nozzle-outlet total pressure, and gas flow by means of the following equation:

$$T_j = T_8 = \frac{g(\gamma_8 - 1)F_{j,s}^2}{2R\gamma_8 W_g^2 C_j^2\left[1 - \left(\frac{p_0}{p_8}\right)^{\frac{\gamma_8 - 1}{\gamma_8}}\right]} \qquad (14)$$

Values of C_j were obtained from figure 19(b); values of γ_8 were based on an estimated exhaust-gas temperature obtained from the scale jet thrust.

Combustion efficiency. - Tail-pipe combustion efficiency was obtained from the ratio of actual enthalpy rise of the gas through the tail-pipe burner to the theoretical enthalpy rise that would result from complete combustion of the tail-pipe-burner fuel. The following equation assumes that the engine fuel was completely burned in the engine combustors:

$$\eta_{b,t} = \frac{3600\, W_{g,8}\Delta H_{g,t}}{W_{f,t}h_{c,t}}$$

$$= \frac{3600\, W_{a,3}H_a\Big]_1^8 + W_{f,e}H_{f,e}\Big]_m^8 + W_{f,t}H_{f,t}\Big]_m^8 - W_{f,e}h_{c,e}}{W_{f,t}h_{c,t}} \qquad (15)$$

The enthalpy of the products of combustion was determined from the charts of reference 6. The effect of dissociation of the gas on combustion efficiency has not been taken into account, inasmuch as this effect is considered negligible for temperatures up to 3600° R.

REFERENCES

1. Fleming, William A., and Wallner, Lewis E.: Altitude-Wind-Tunnel Investigation of Tail-Pipe Burning with a Westinghouse X24C-4B Axial-Flow Turbojet Engine. NACA RM E8J25e, 1948.

2. Conrad, E. William, and Prince, William R.: Altitude Performance and Operational Characteristics of 29-Inch-Diameter Tail-Pipe Burner with Several Fuel Systems and Flame Holders on J35 Turbojet Engine. NACA RM E9G08, 1949.

3. Thorman, H. Carl, and Campell, Carl E.: Altitude-Wind-Tunnel Investigation of Tail-Pipe Burner with Converging Conical Burner Section on J35-A-5 Turbojet Engine. NACA RM E9I16, 1950.

4. Golladay, Richard L., and Bloomer, Harry E.: Altitude Performance and Operational Characteristics of 29-Inch-Diameter Tail-pipe Burner with Several Fuel Systems and Fuel-Cooled Stage-Type Flame Holders on J35-A-5 Turbojet Engine. NACA RM E50A19, 1950.

5. Jansen, Emmert T., and Thorman, H. Carl: Altitude Performance Characteristics of Tail-Pipe Burner with Variable-Area Exhaust Nozzle. NACA RM E50E29, 1950.

6. Turner, L. Richard, and Bogart, Donald: Constant-Pressure Combustion Charts Including Effects of Diluent Addition. NACA Rep. 937, 1949. (Formerly NACA TNs 1086 and 1655.)

TABLE I - PERFORMANCE DATA FOR J47 TURBOJET

Run	Altitude (ft)	Flight Mach number M_0	Ambient pressure p_0 (lb/sq ft abs.)	Engine-inlet total pressure P_1 (lb/sq ft abs.)	Engine-inlet total temperature T_1 (°R)	Engine fuel flow $W_{f,e}$ (lb/hr)	Tail-pipe fuel flow $W_{f,t}$ (lb/hr)	Jet thrust F_j (lb)	Net thrust F_n (lb)	Air flow W_a (lb/sec)	Specific fuel consumption W_f/F_n (lb/(hr)(lb thrust))
Configuration A											
1	25,000	0.200	780	802	513	2240	3150	2358	2112	36.08	2.552
2	25,000	.225	780	808	505	2240	3400	2377	2093	36.89	2.694
3	25,000	.200	783	807	509	2240	3700	2400	2138	36.55	2.778
4	35,000	.210	493	510	511	1400	2450	1451	1279	22.92	3.010
5	35,000	.210	496	512	504	1390	2760	1453	1286	23.14	3.227
6	35,000	.210	493	509	495	1400	3000	1405	1238	23.27	3.554
Configuration B											
1	25,000	0.225	780	808	498	2210	3100	2459	2173	37.45	2.442
2	25,000	.225	781	809	497	2165	5055	2519	2234	37.37	3.232
3	25,000	.205	781	805	506	2210	4080	2538	2276	36.58	2.762
4	25,000	.220	777	804	502	2140	4080	2483	2204	36.97	2.820
5	25,000	.205	781	805	503	2150	6220	2459	2195	36.99	3.813
6	35,000	.205	493	508	504	1390	2050	1439	1276	23.22	2.696
7	35,000	.230	493	512	499	1400	2700	1517	1331	23.44	3.080
8	35,000	.210	498	514	502	1300	3300	1436	1267	23.40	3.631
9	35,000	.210	494	510	503	1390	3370	1480	1313	23.12	3.625
10	35,000	.210	499	515	499	1390	3550	1488	1319	23.52	3.745
11	35,000	.210	500	516	504	1350	4000	1464	1295	23.45	4.131
Configuration C											
1	25,000	.210	781	805	514	2080	3850	2264	1999	36.73	2.956
2	25,000	.225	781	809	515	2120	4320	2485	2201	36.58	2.926
3	25,000	.230	762	792	505	2130	4450	2467	2179	36.04	3.020
4	25,000	.215	781	807	513	2250	4510	2562	2281	36.54	2.964
5	25,000	.225	781	809	501	2300	5000	2739	2455	37.03	2.973
6	25,000	.230	781	812	505	2300	5450	2819	2520	36.94	3.075
7	25,000	.220	781	808	518	2200	5700	2557	2277	36.41	3.469
8	35,000	.225	493	511	514	1420	2390	1534	1353	23.06	2.816
9	35,000	.225	494	512	504	1430	2850	1569	1390	23.32	3.079
10	35,000	.215	493	510	506	1340	2850	1462	1290	23.04	3.248
11	35,000	.210	493	509	514	1360	2860	1468	1301	22.87	3.241
12	35,000	.210	493	509	510	1410	3400	1507	1341	22.86	3.587
13	35,000	.215	493	510	497	1410	3400	1503	1328	23.66	3.622
14	35,000	.225	493	511	499	1360	3400	1549	1368	23.39	3.479
15	35,000	.200	493	508	508	1350	3540	1479	1318	22.90	3.710
Configuration E											
1	25,000	0.225	780	808	504	2200	2450	2246	1962	36.93	2.370
2	25,000	.235	778	808	505	2210	3000	2327	2030	37.18	2.566
3	25,000	.225	781	808	503	2350	4000	2567	2288	36.86	2.775
4	25,000	.236	778	808	499	2300	4000	2568	2273	37.13	2.772
5	25,000	.225	781	808	501	2150	4000	2400	2118	37.33	2.903
6	25,000	.230	776	805	497	2400	4700	2663	2376	37.21	2.988
7	35,000	.235	493	512	506	1470	2000	1518	1331	23.44	2.607
8	35,000	.235	493	512	505	1400	2000	1426	1239	23.46	2.744
9	35,000	.230	499	517	502	1490	2500	1562	1380	23.68	2.891
10	35,000	.250	493	515	501	1390	2500	1486	1278	23.71	3.045
11	35,000	.225	494	512	499	1480	2800	1578	1399	23.44	3.059

NACA

1362

[redacted]

1362

ENGINE WITH TAIL-PIPE BURNER OPERATIVE

Total fuel-air ratio f/a	Tail-pipe fuel-air ratio $(f/a)_t$	Tail-pipe combustion efficiency $\eta_{b,t}$	Turbine-outlet total pressure P_6 (lb/sq ft abs.)	Turbine-outlet total temperature T_6 (°R)	Combustion-chamber-inlet static pressure p_7 (lb/sq ft abs.)	Exhaust-nozzle total pressure P_8 (lb/sq ft abs.)	Exhaust-gas total temperature T_j (°R)	Combustion-chamber-inlet velocity V_7 (ft/sec)	Augmented thrust ratio	Run
Configuration A										
0.0423	0.0335	0.584	1485	1757	1340	1357	2560	496	1.175	1
.0433	.0351	.532	1480	1745	1317	1352	2499	511	1.170	2
.0459	.0387	.553	1480	1742	1318	1350	2604	506	1.196	3
.0474	.0407	.467	923	1766	823	832	2492	517	1.146	4
.0506	.0451	.463	910	1729	811	818	2544	520	1.172	5
.0534	.0488	.328	907	1710	810	816	2326	520	1.125	6
Configuration B										
0.0408	0.0312	0.679	1481	1684	1309	1350	2582	514	1.219	1
.0543	.0507	.577	1455	1677	1311	1307	2848	515	1.260	2
.0483	.0424	.667	1472	1736	1316	1337	2866	522	1.280	3
.0473	.0413	.652	1440	1677	1282	1302	2791	522	1.281	4
.0636	.0631	.443	1449	1710	1302	1298	2750	527	1.250	5
.0415	.0333	.573	906	1736	803	818	2491	533	1.149	6
.0499	.0435	.516	923	1708	829	831	2604	517	1.200	7
.0552	.0520	.460	890	1673	791	790	2594	532	1.195	8
.0578	.0551	.424	910	1731	815	814	2611	530	1.191	9
.0590	.0568	.414	914	1705	817	814	2594	530	1.191	10
.0641	.0636	.358	908	1705	809	810	2530	536	1.185	11
Configuration C										
.0450	.0390	.582	1408	1662	1264	1261	2601	506	1.203	1
.0492	.0444	.552	1476	1709	1301	1381	2674	503	1.264	2
.0516	.0465	.624	1419	1675	1266	1290	2887	503	1.306	3
.0523	.0472	.605	1481	1738	1327	1353	2889	505	1.282	4
.0558	.0518	.730	1482	1732	1331	1346	3242	511	1.372	5
.0593	.0567	.754	1489	1755	1339	1349	3413	515	1.404	6
.0606	.0595	.576	1466	1749	1321	1307	3047	514	1.300	7
.0466	.0396	.587	927	1740	830	845	2688	508	1.220	8
.0518	.0466	.564	922	1717	836	836	2782	508	1.255	9
.0513	.0463	.548	885	1664	803	794	2714	506	1.240	10
.0521	.0471	.468	908	1720	817	823	2595	510	1.199	11
.0594	.0568	.357	941	1734	849	858	2508	498	1.192	12
.0573	.0542	.383	914	1686	827	825	2503	514	1.193	13
.0574	.0544	.533	898	1663	818	806	2839	508	1.285	14
.0602	.0581	.455	892	1675	800	799	2728	511	1.248	15
Configuration E										
0.0356	0.0251	0.457	1465	1681	1342	1385	2182	483	1.129	1
.0396	.0305	.462	1463	1683	1342	1382	2289	489	1.165	2
.0487	.0421	.544	1513	1730	1395	1422	2682	484	1.256	3
.0480	.0413	.571	1492	1694	1376	1400	2698	484	1.276	4
.0466	.0401	.502	1443	1656	1322	1343	2504	494	1.230	5
.0539	.0492	.532	1514	1748	1398	1417	2796	495	1.280	6
.0418	.0328	.480	940	1735	865	885	2394	496	1.171	7
.0408	.0322	.410	913	1674	836	854	2241	494	1.142	8
.0476	.0406	.454	949	1665	872	889	2490	479	1.227	9
.0462	.0396	.440	908	1728	833	845	2391	520	1.171	10
.0515	.0460	.447	943	1722	867	881	2561	495	1.226	11

NACA

TABLE I - PERFORMANCE DATA FOR J47 TURBOJET

Run	Altitude (ft)	Flight Mach number M_0	Ambient pressure p_0 (lb/sq ft abs.)	Engine-inlet total pressure p_1 (lb/sq ft abs.)	Engine-inlet total temperature T_1 (°R)	Engine fuel flow $W_{f,e}$ (lb/hr)	Tail-pipe fuel flow $W_{f,t}$ (lb/hr)	Jet thrust F_j (lb)	Net thrust F_n (lb)	Air flow W_a (lb/sec)	Specific fuel consumption W_f/F_n (lb/(hr)(lb thrust))
Configuration D											
1	25,000	0.200	785	808	505	2300	2820	2456	2204	36.43	2.330
2	25,000	.215	776	803	501	2310	3300	2856	2281	36.41	2.468
3	25,000	.210	774	800	506	2190	3300	2411	2141	36.13	2.573
4	25,000	.210	781	807	501	2380	3300	2597	2327	36.83	2.448
5	25,000	.215	777	804	503	2210	3750	2509	2234	36.42	2.677
6	25,000	.215	781	808	505	2300	3750	2534	2256	36.67	2.690
7	25,000	.205	781	806	496	2260	4000	2575	2310	36.93	2.715
8	25,000	.225	778	805	506	2155	4000	2474	2197	36.56	2.806
9	25,000	.215	773	799	503	2244	4400	2631	2361	36.19	2.816
10	25,000	.210	778	804	499	2300	4800	2731	2464	36.53	2.889
11	25,000	.530	781	945	501	2540	4800	3355	2597	43.20	2.826
12	25,000	.520	831	996	510	2710	5690	3575	2796	45.02	3.018
13	25,000	.520	799	960	498	2670	5690	3571	2810	44.23	2.985
14	25,000	.520	777	934	503	2700	5700	3567	2832	42.49	2.966
15	25,000	.520	781	938	504	2660	5700	3553	2814	42.77	2.970
16	25,000	.515	803	961	503	2660	6050	3613	2856	44.22	3.060
17	25,000	.515	781	936	504	2610	6050	3525	2759	42.62	3.117
18	25,000	.825	781	1220	505	3200	5200	4598	3133	55.28	2.681
19	25,000	.820	785	1219	501	3620	6000	5199	3719	56.43	2.586
20	25,000	.820	796	1241	504	3350	6100	4987	3474	57.28	2.720
21	25,000	.820	788	1228	500	3340	7000	5127	3630	56.96	2.848
22	25,000	.840	781	1236	501	3340	7200	5286	3759	57.10	2.803
23	35,000	.200	491	506	500	1440	2200	1558	1397	22.68	2.616
24	35,000	.205	493	509	512	1287	2300	1384	1218	22.85	2.949
25	35,000	.215	493	510	504	1360	2300	1460	1288	23.01	2.841
26	35,000	.230	493	512	505	1310	2300	1442	1258	23.05	2.869
27	35,000	.215	493	510	507	1390	2500	1509	1339	22.75	2.905
28	35,000	.210	493	509	500	1360	2500	1500	1335	22.86	2.891
29	35,000	.210	494	510	502	1410	2500	1545	1330	22.85	2.939
30	35,000	.220	492	509	497	1450	2500	1555	1382	22.97	2.858
31	35,000	.205	493	509	509	1373	2500	1493	1327	22.92	2.923
32	35,000	.200	493	508	501	1400	2500	1541	1380	22.93	2.836
33	35,000	.190	498	512	504	1440	2500	1543	1387	23.06	2.853
34	35,000	.200	493	508	501	1410	2700	1547	1386	22.93	2.976
35	35,000	.205	493	509	505	1430	2700	1561	1395	23.04	2.973
36	35,000	.215	491	508	497	1450	2900	1611	1436	23.23	3.039
37	35,000	.205	493	509	502	1412	2900	1548	1382	23.08	3.124
38	35,000	.220	489	506	497	1430	2900	1570	1398	22.87	3.097
39	35,000	.210	493	509	499	1440	2900	1556	1390	23.10	3.122
40	45,000	.225	292	303	502	860	1080	797	690	13.66	2.776
41	45,000	.345	296	321	503	890	1240	877	710	14.47	3.000
42	45,000	.275	296	312	495	860	1340	889	761	13.79	2.891
43	45,000	.225	294	305	507	820	1360	777	671	13.63	3.243
44	45,000	.230	315	327	507	900	1350	853	737	14.67	3.057
45	45,000	.220	304	315	506	895	1500	871	765	14.01	3.138
46	45,000	.230	310	322	503	895	2100	886	771	14.37	3.889

ENGINE WITH TAIL-PIPE BURNER OPERATIVE. CONCLUDED

Total fuel-air ratio f/a	Tail-pipe fuel-air ratio $(f/a)_t$	Tail-pipe combustion efficiency $\eta_{b,t}$	Turbine-outlet total pressure P_6 (lb/sq ft abs.)	Turbine-outlet total temperature T_6 (°R)	Combustion-chamber-inlet static pressure p_7 (lb/sq ft abs.)	Exhaust-nozzle total pressure P_8 (lb/sq ft abs.)	Exhaust-gas total temperature T_j (°R)	Combustion-chamber-inlet velocity V_7 (ft/sec)	Augmented thrust ratio	Run
Configuration D										
0.0398	0.0299	0.772	1510	1742	1382	1370	2730	481	1.213	1
.0435	.0351	.798	1501	1727	1376	1362	2912	481	1.272	2
.0429	.0348	.749	1458	1705	1327	1306	2810	487	1.239	3
.0437	.0349	.756	1534	1750	1408	1393	2860	481	1.251	4
.0463	.0392	.760	1469	1708	1342	1315	2956	489	1.280	5
.0466	.0394	.698	1502	1740	1375	1350	2871	490	1.251	6
.0479	.0414	.709	1493	1706	1367	1344	2926	487	1.282	7
.0476	.0412	.716	1452	1716	1325	1296	2925	500	1.264	8
.0519	.0466	.777	1478	1729	1355	1320	3202	490	1.336	9
.0550	.0507	.767	1509	1752	1393	1345	3297	490	1.348	10
.0482	.0419	.750	1707	1661	1561	1541	3002	485	1.410	11
.0529	.0482	.735	1827	1703	1690	1618	3152	484	1.414	12
.0536	.0490	.748	1776	1702	1640	1578	3196	488	1.430	13
.0560	.0521	.756	1759	1753	1617	1590	3312	490	1.450	14
.0554	.0513	.762	1748	1753	1604	1577	3295	497	1.446	15
.0558	.0521	.740	1787	1699	1650	1587	3257	485	1.455	16
.0550	.0511	.656	1738	1705	1605	1543	3049	505	1.388	17
.0433	.0356	.715	2201	1641	2007	1994	2766	472	1.385	18
.0484	.0416	.858	2372	1766	2185	2169	3180	480	1.433	19
.0469	.0404	.767	2258	1653	2066	2046	2984	481	1.460	20
.0516	.0466	.756	2261	1651	2070	2037	3137	479	1.517	21
.0524	.0478	.828	2260	1663	2069	2034	3301	485	1.567	22
.0453	.0374	.793	922	1737	840	825	2976	495	1.265	23
.0443	.0373	.656	878	1681	796	767	2692	508	1.178	24
.0449	.0376	.638	903	1726	821	801	2702	511	1.192	25
.0442	.0371	.657	892	1677	813	792	2694	501	1.209	26
.0482	.0418	.657	914	1727	835	814	2847	499	1.238	27
.0492	.0412	.693	901	1696	823	799	2883	498	1.249	28
.0498	.0418	.702	918	1730	840	817	2939	499	1.212	29
.0485	.0419	.671	921	1738	837	823	2886	505	1.248	30
.0477	.0412	.708	899	1696	819	790	2917	502	1.241	31
.0480	.0415	.756	905	1694	830	801	3009	496	1.277	32
.0482	.0416	.689	924	1734	847	820	2909	501	1.240	33
.0506	.0449	.675	916	1729	839	810	2958	502	1.255	34
.0506	.0448	.673	914	1741	837	813	2958	509	1.256	35
.0528	.0479	.661	930	1730	854	822	3002	501	1.274	36
.0528	.0478	.613	919	1730	841	809	2908	505	1.245	37
.0534	.0487	.618	921	1703	846	819	2936	490	1.276	38
.0530	.0481	.593	921	1739	847	819	2877	506	1.244	39
.0395	.0297	.401	535	1743	484	484	2230	514	1.076	40
.0417	.0328	.450	563	1770	505	498	2347	529	1.084	41
.0451	.0373	.629	554	1755	495	489	2708	512	1.165	42
.0450	.0376	.361	525	1694	472	472	2254	513	1.077	43
.0434	.0352	.358	572	1708	517	519	2238	508	1.087	44
.0484	.0416	.455	557	1758	505	498	2522	514	1.152	45
.0590	.0562	.344	564	1744	513	504	2470	520	1.156	46

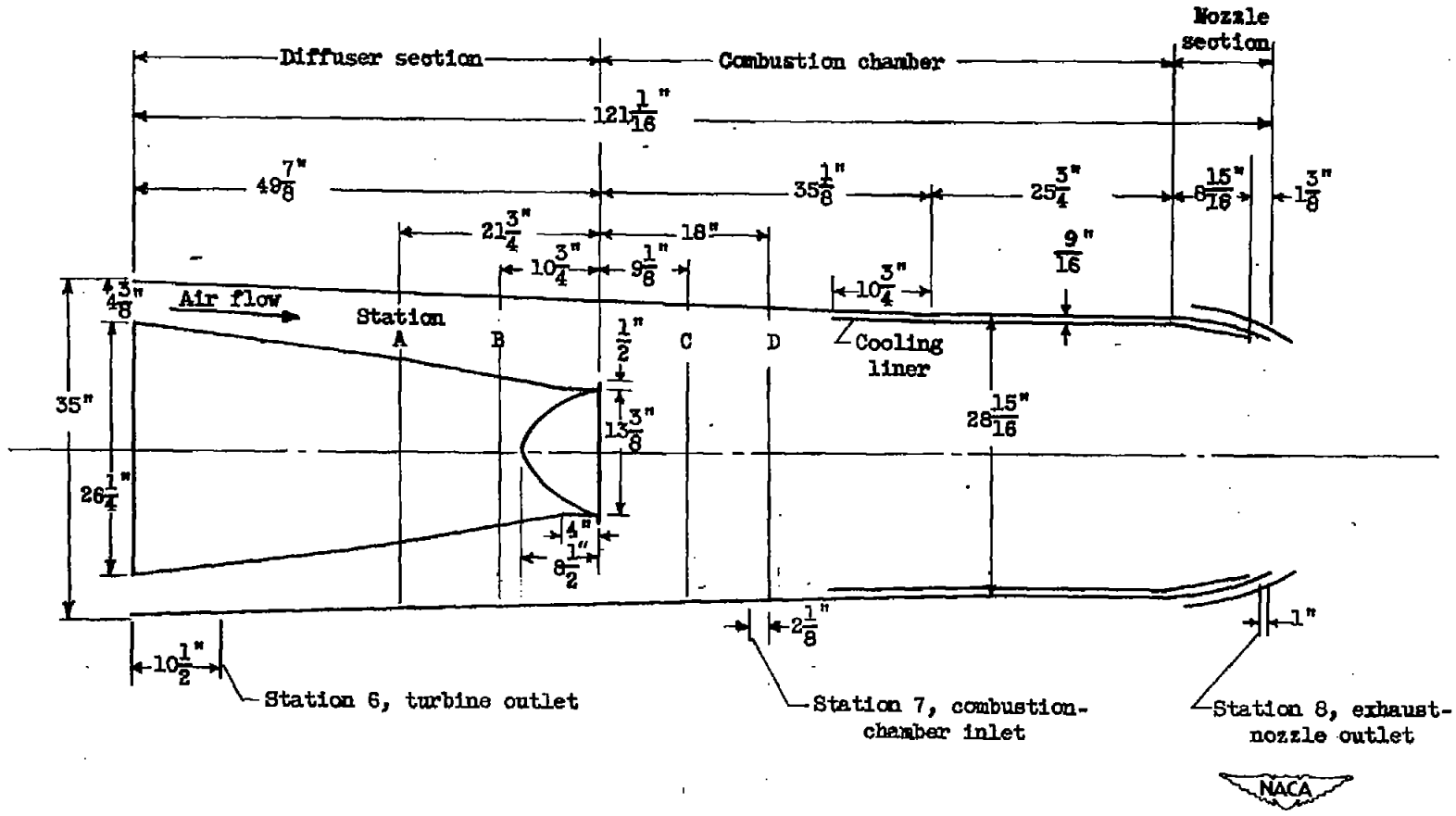

Figure 1. - Cross-section of tail-pipe burner showing stations at which fuel-spray bars, flame holders, and instrumentation were installed.

(a) Open position.

Figure 2. - Variable-area exhaust nozzle

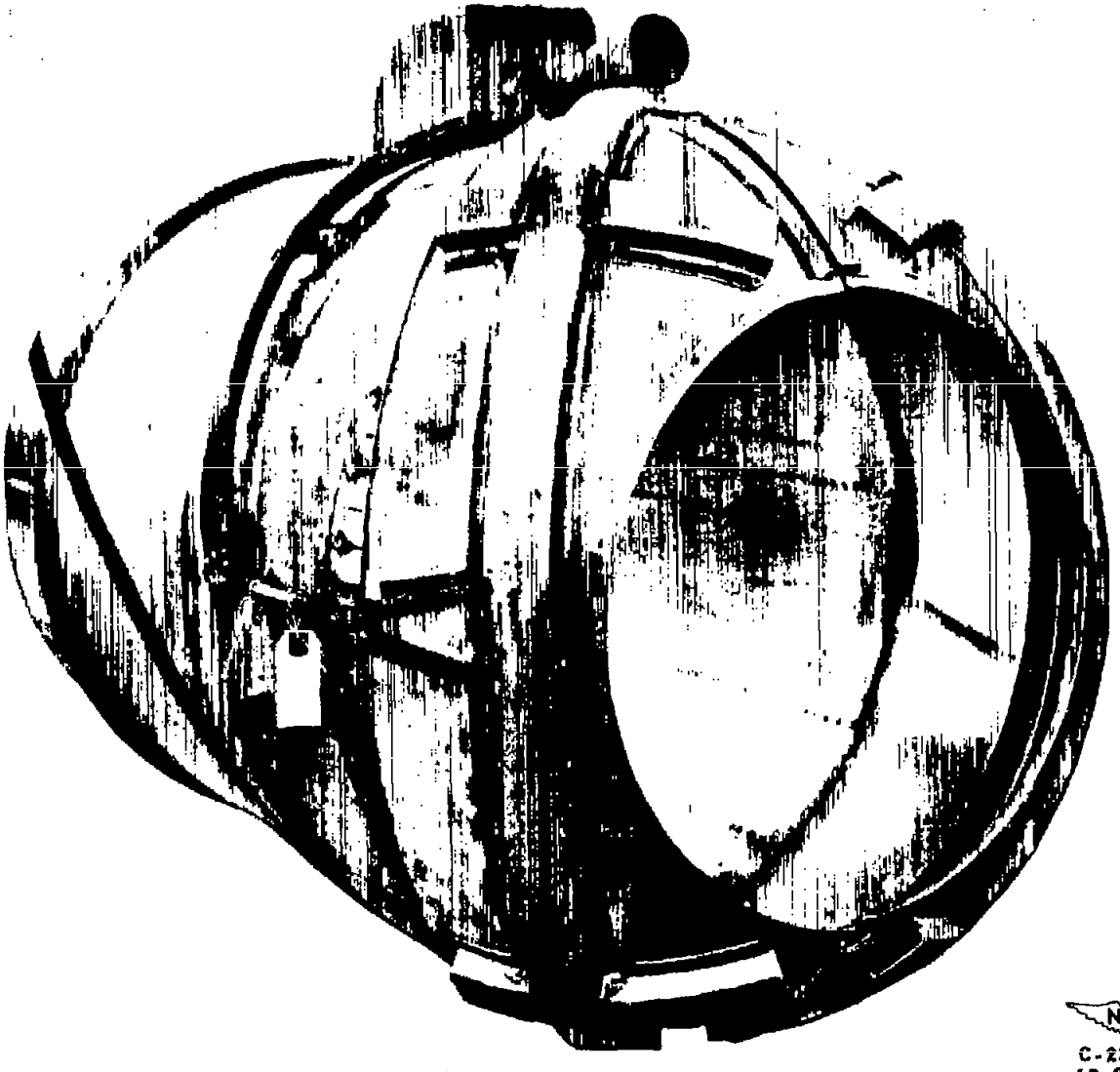

NACA
C-22463
10-27-48

(b) Closed position.

Figure 2. - Concluded. Variable-area exhaust nozzle.

Figure 3. - Installation of turbojet engine with tail-pipe burner and variable-area exhaust nozzle in altitude wind tunnel.

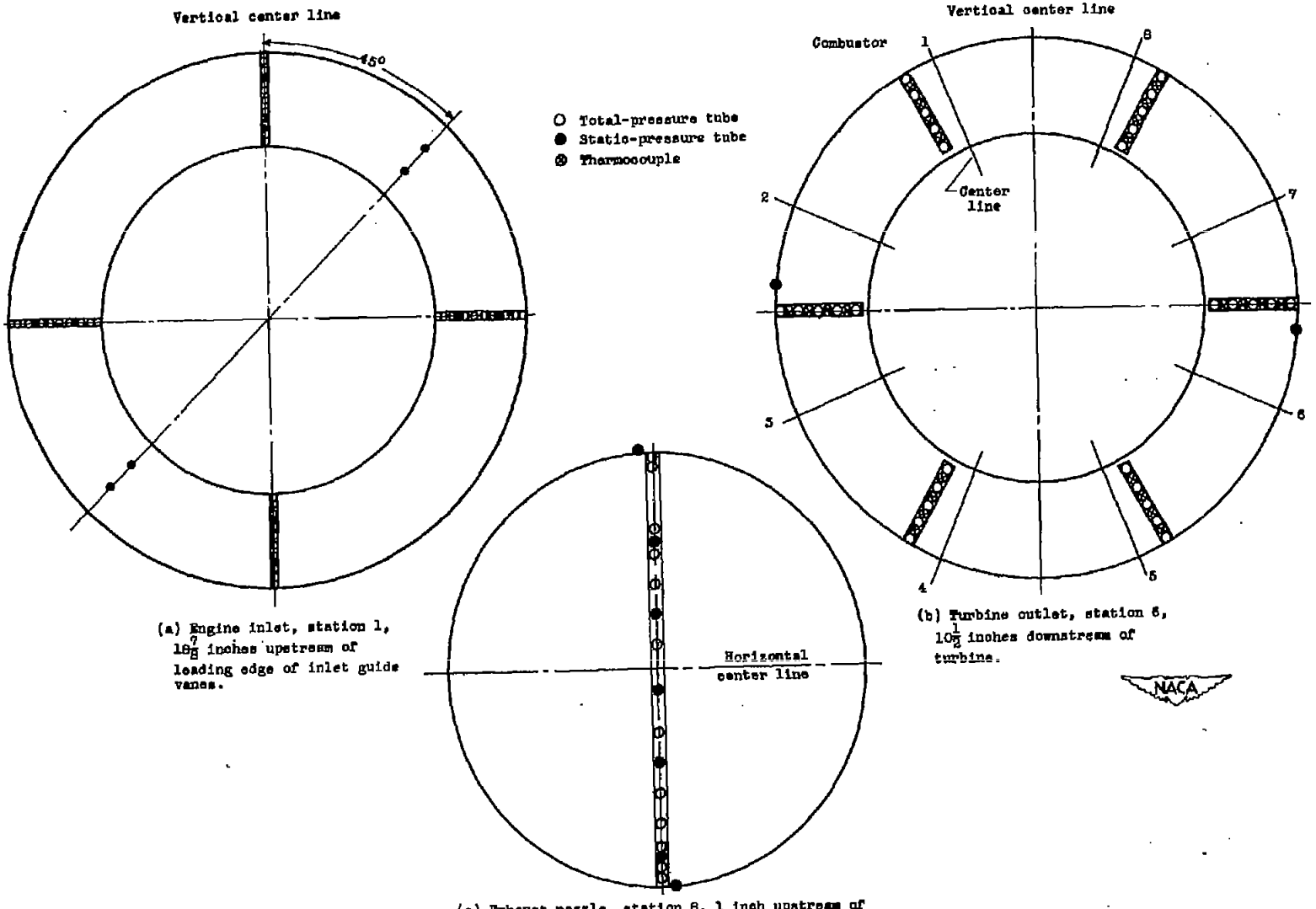

(a) Engine inlet, station 1, $18\frac{7}{8}$ inches upstream of leading edge of inlet guide vanes.

(b) Turbine outlet, station 6, $10\frac{1}{2}$ inches downstream of turbine.

(c) Exhaust nozzle, station 8, 1 inch upstream of fixed portion of exhaust nozzle.

Figure 4. - Cross section of measuring stations showing location of instrumentation. Viewed looking downstream.

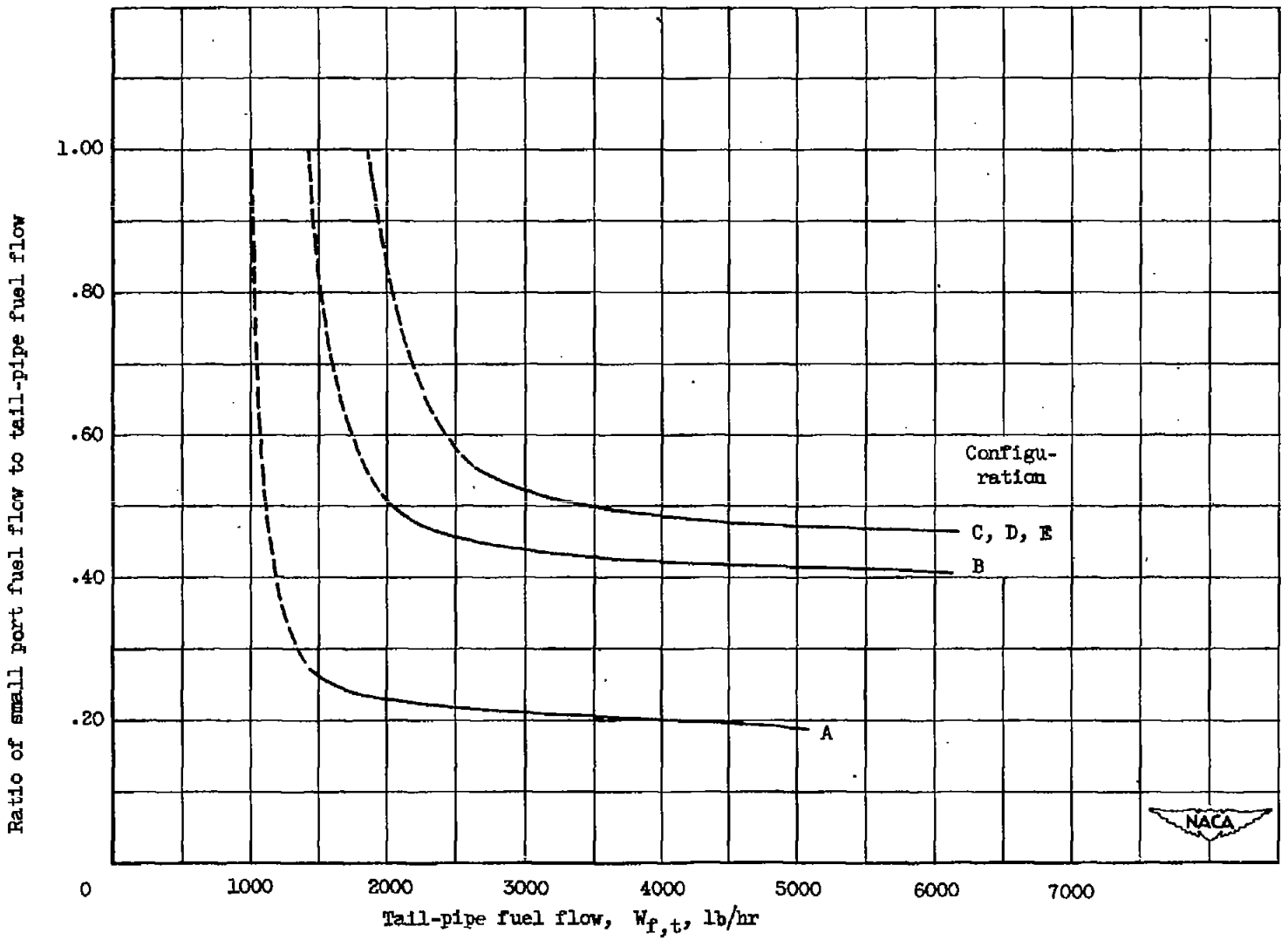

Figure 5. - Schedules for flow divider used for each configuration.

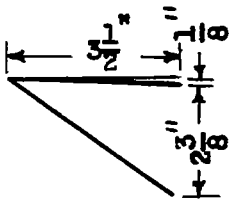

Detail A-A

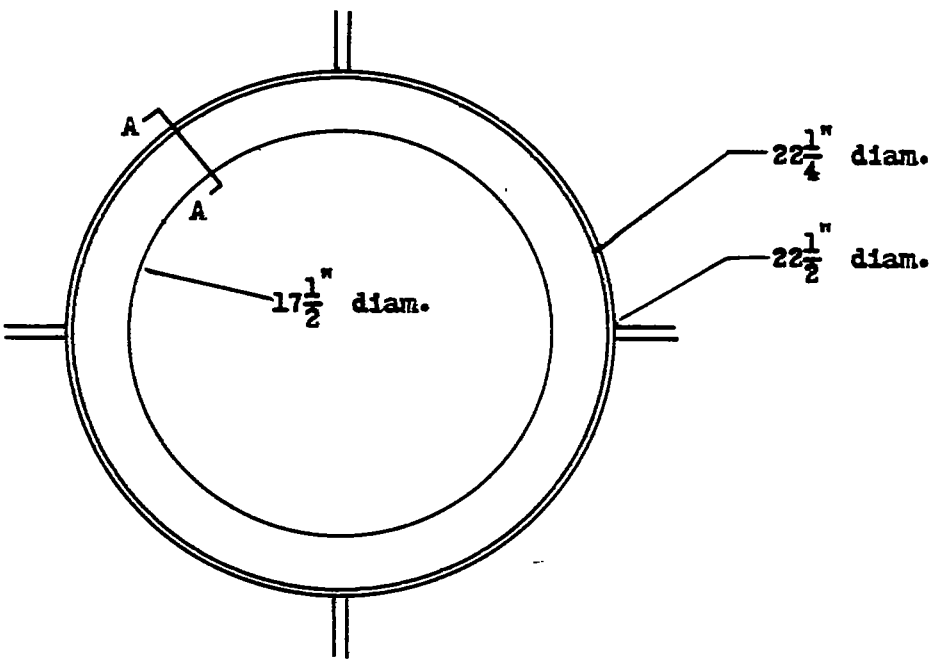

Flame holder attached at station D (fig. 1)

NACA

Figure 6. - Details of unsymmetric V-gutter flame holder.

[redacted]

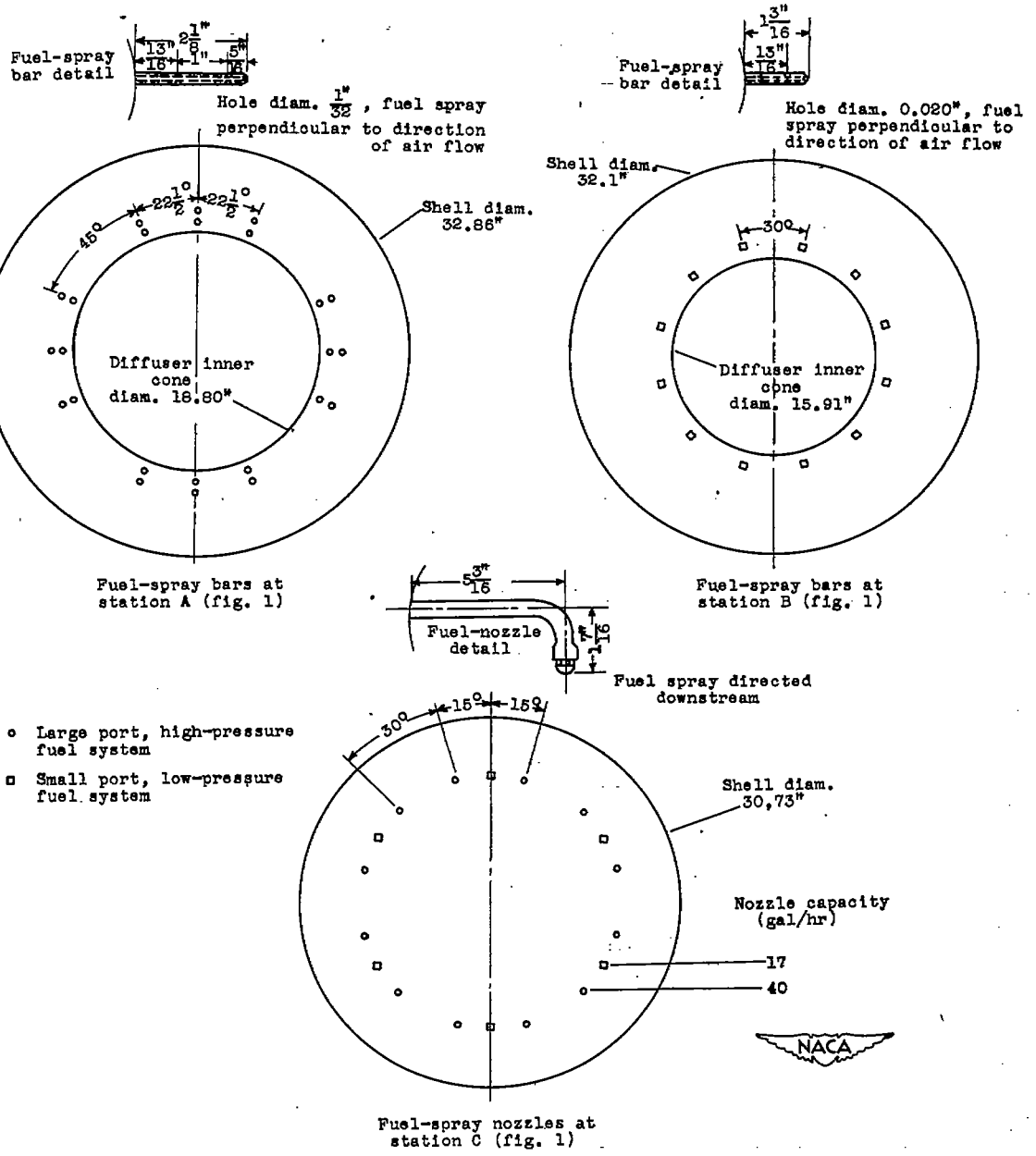

Figure 7. - Details of fuel system used for configuration A.

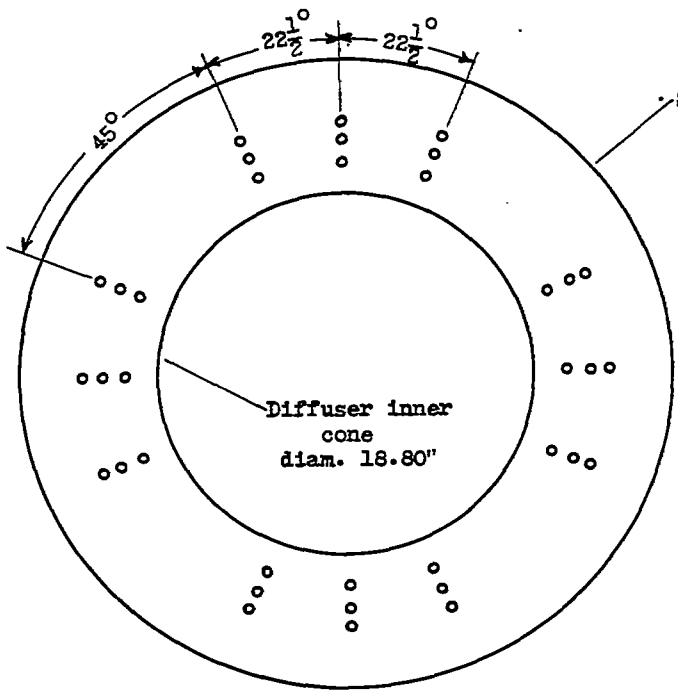

Fuel-spray bars at
station A (fig. 1)

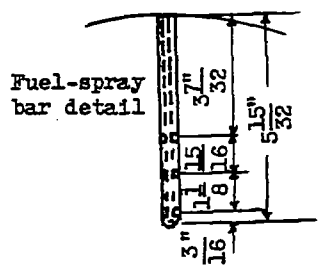

Hole diam. 1/32", fuel spray
perpendicular to air flow

○ Large port, high-pressure fuel system

□ Small port, low-pressure fuel system

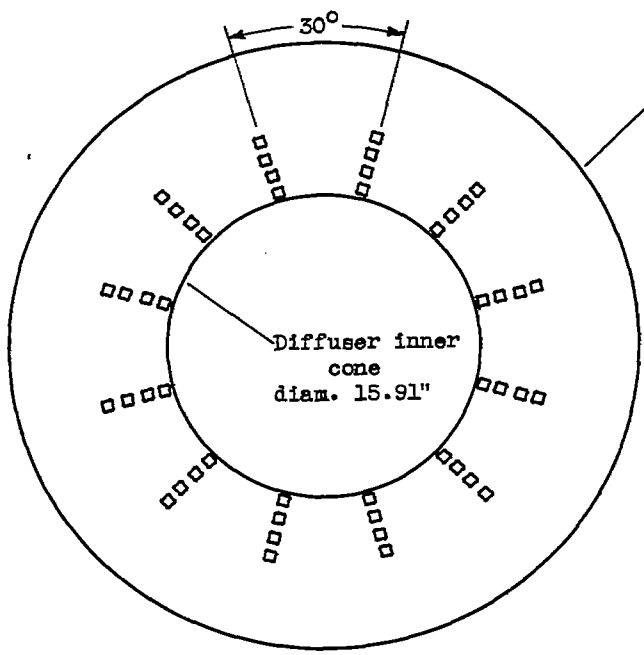

Fuel-spray bars at
station B (fig. 1)

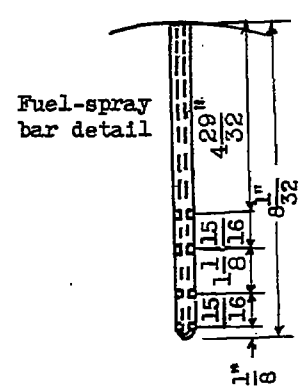

Hole diam. 0.020", fuel spray
perpendicular to air flow

NACA

Figure 8. - Details of fuel system used for configuration B.

[redacted]

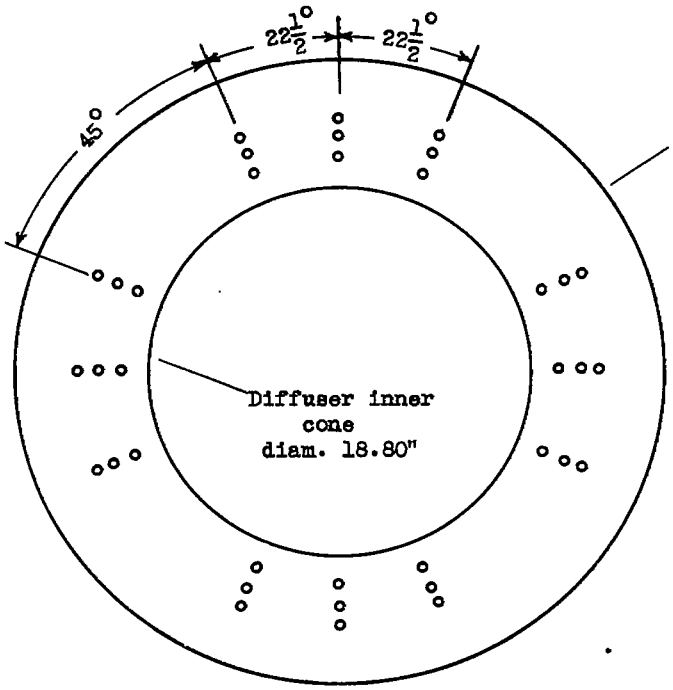

Fuel spray bars at station A (fig. 1)

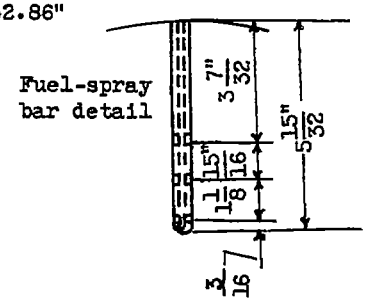

Hole diam. 1/32", fuel spray perpendicular to air flow

○ Large port, high-pressure fuel system

□ Small port, low-pressure fuel system

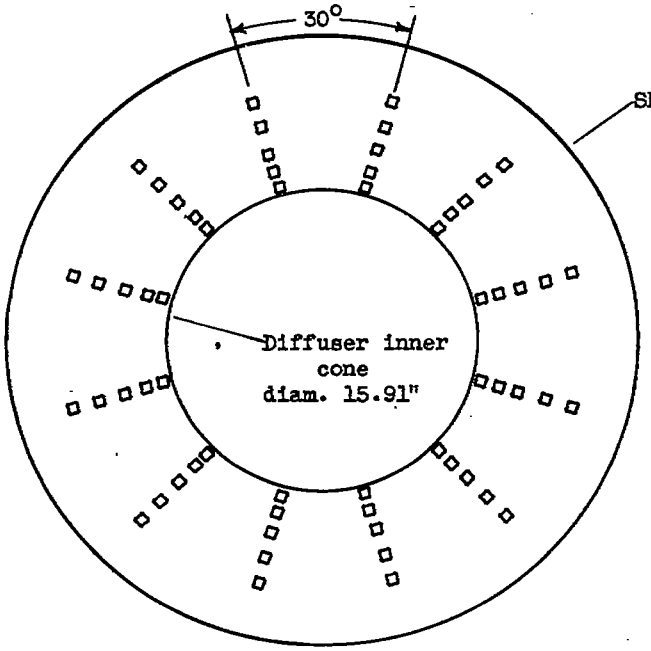

Fuel spray bars at station B (fig. 1)

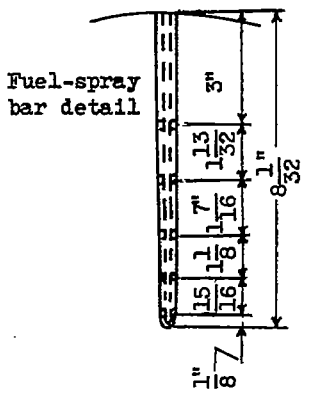

Hole diam. 0.020", fuel spray perpendicular to air flow

NACA

Figure 9. - Details of fuel system used for configuration C, D, and E.

[redacted]

1362

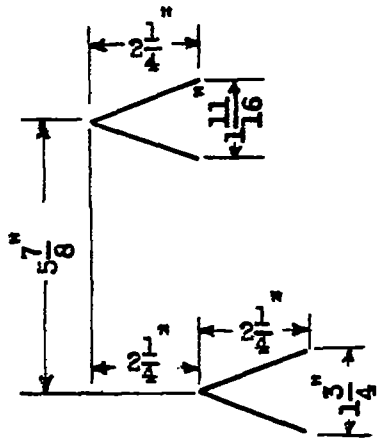

Detail A-A

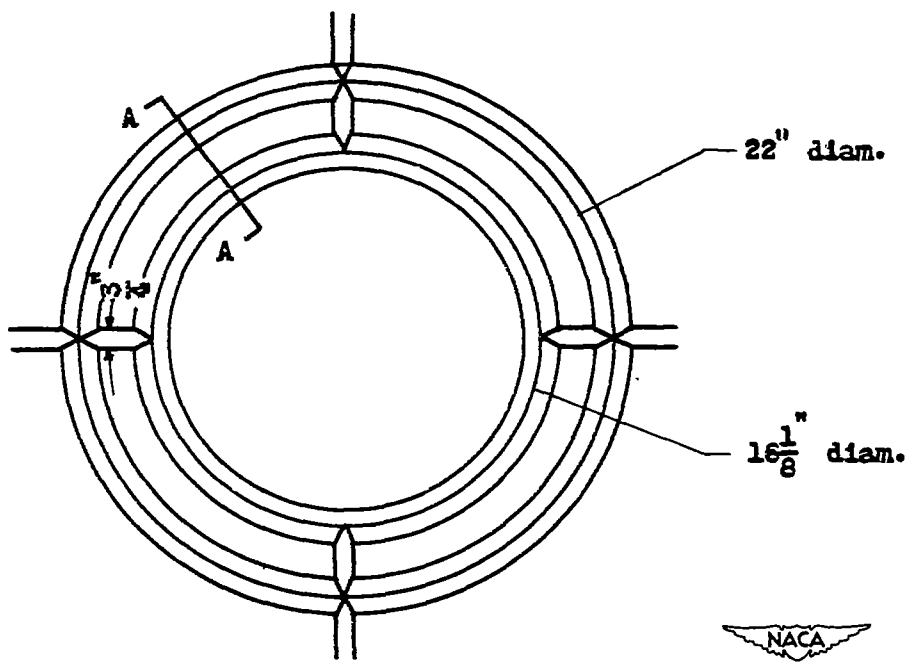

Flame holder attached at station D (fig. 1)

Figure 10. - Details of double V-gutter flame holder.

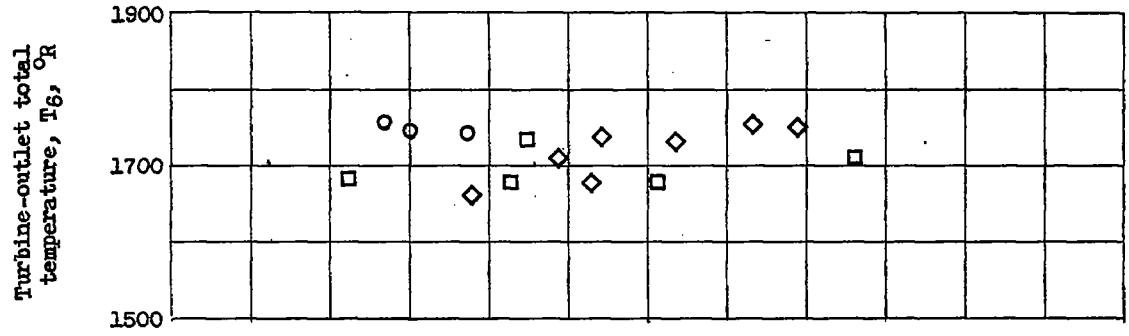

(a) Turbine-outlet total temperature.

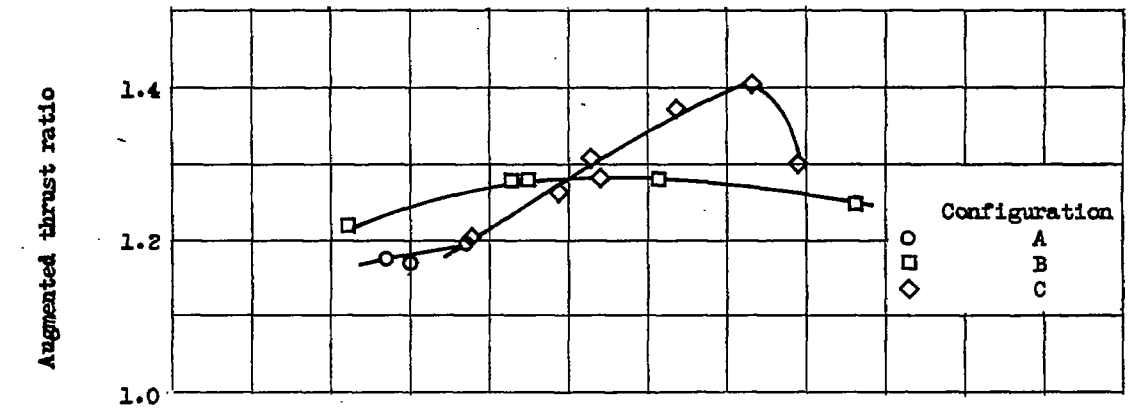

(b) Augmented thrust ratio.

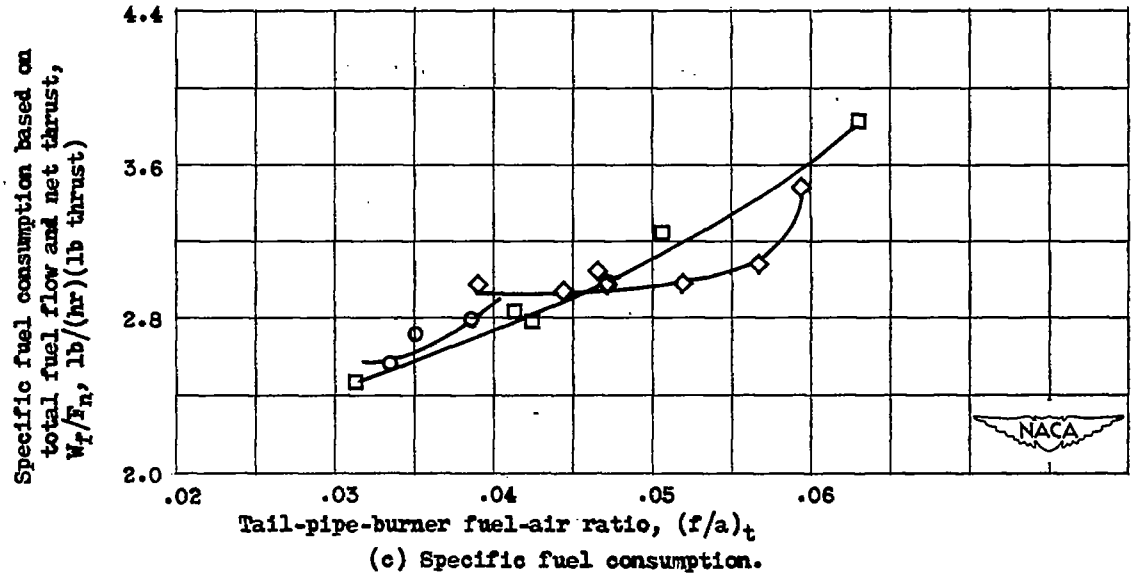

(c) Specific fuel consumption.

Figure 11. - Variation of performance with tail-pipe fuel-air ratio for configurations A, B, and C. Altitude, 25,000 feet; flight Mach number, 0.21; engine speed, 7900 rpm; engine-inlet total temperature, 500° R ± 10°.

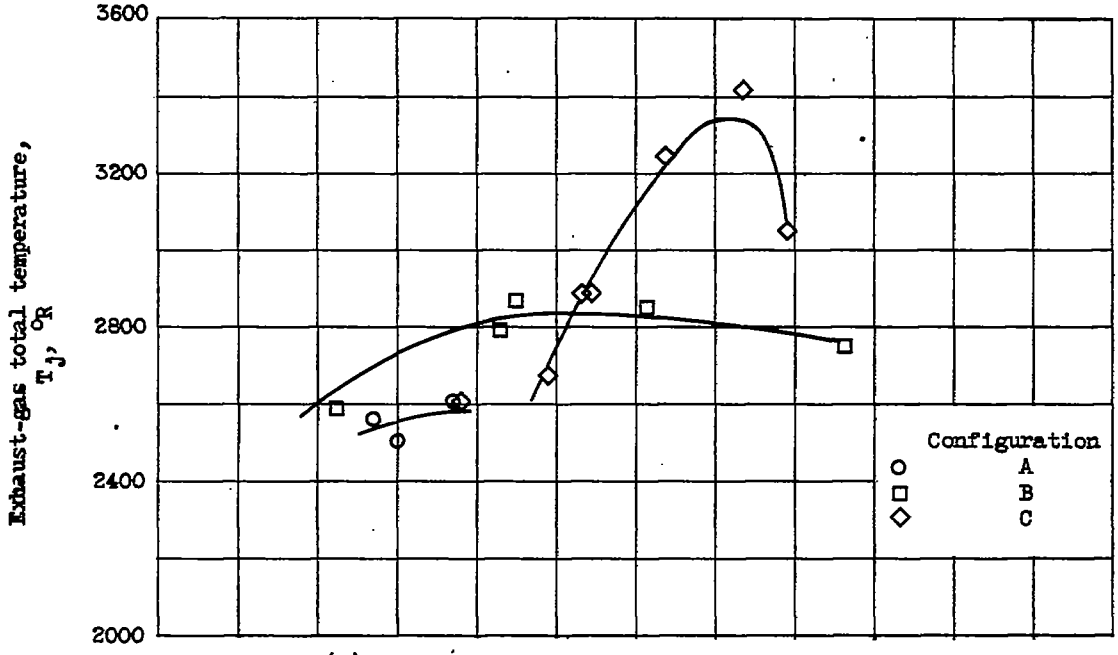

(d) Exhaust-gas total temperature.

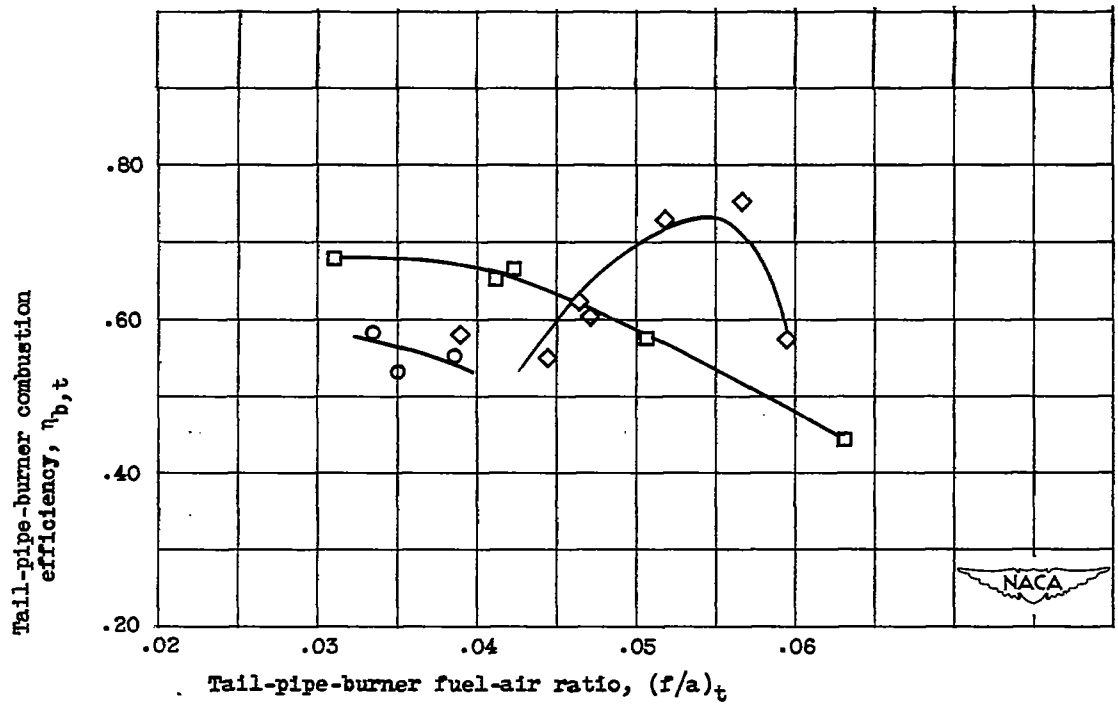

(e) Tail-pipe-burner combustion efficiency.

Figure 11. - Concluded. Variation of performance with tail-pipe fuel-air ratio for configurations A, B, and C. Altitude, 25,000 feet; flight Mach number, 0.21; engine speed, 7900 rpm; engine-inlet total temperature, 500° R ± 10°.

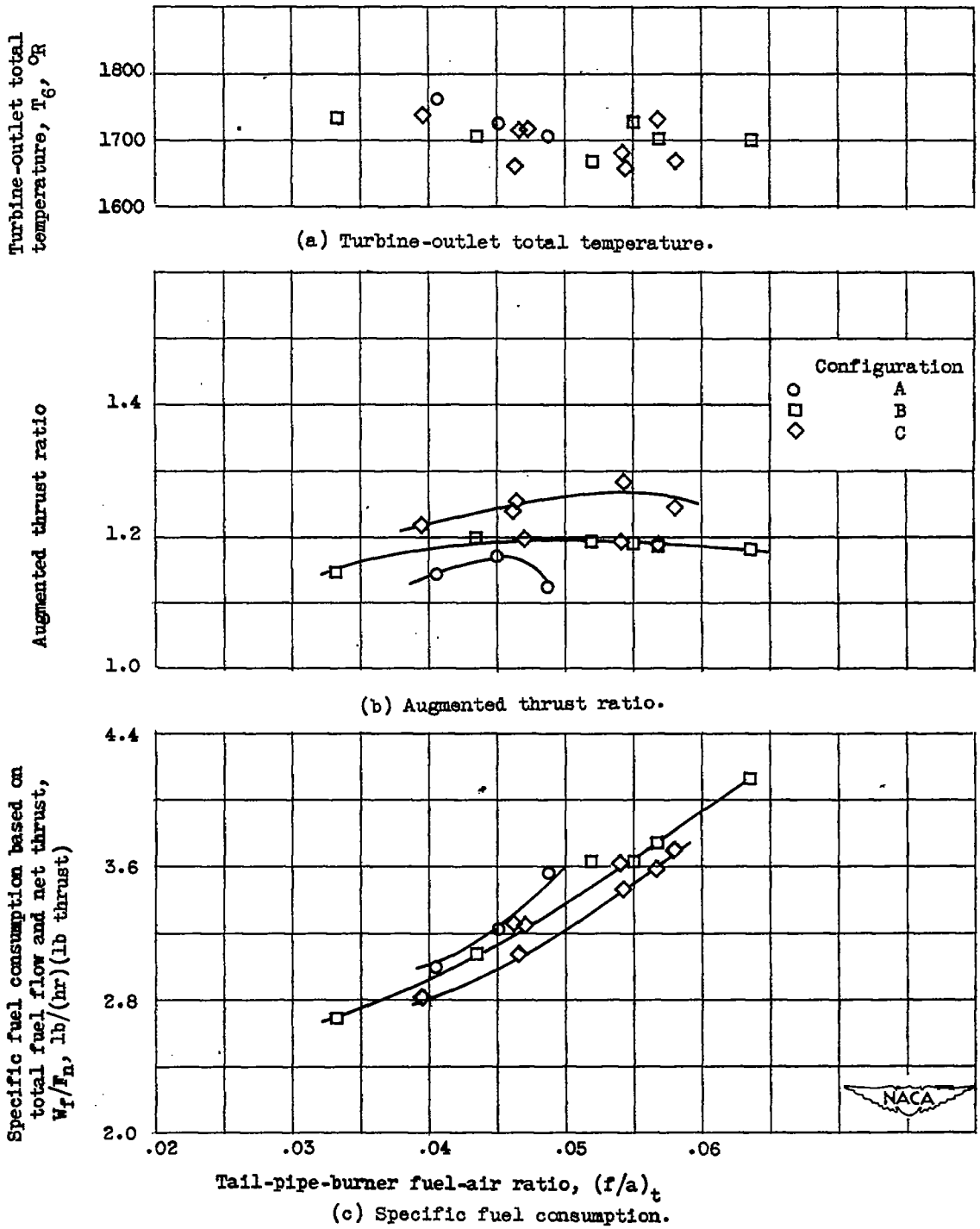

(a) Turbine-outlet total temperature.

(b) Augmented thrust ratio.

(c) Specific fuel consumption.

Figure 12. - Variation of performance with tail-pipe fuel-air ratio for configurations A, B, and C. Altitude, 35,000 feet; flight Mach number, 0.21; engine speed, 7900 rpm; engine-inlet total temperature, 500° R ±10°.

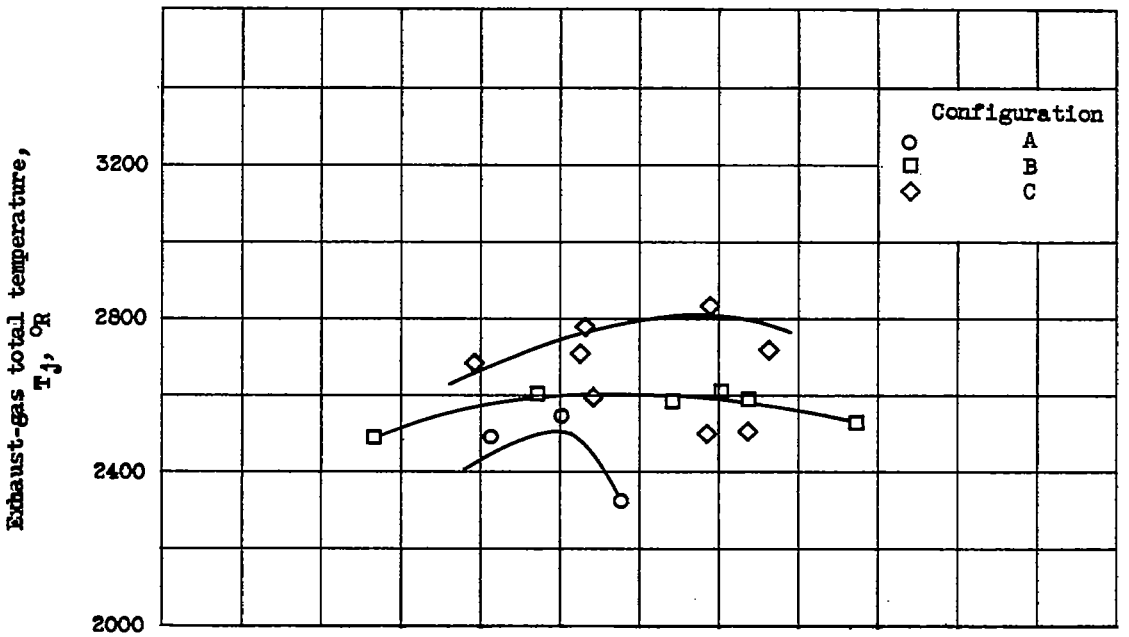

(d) Exhaust-gas total temperatures.

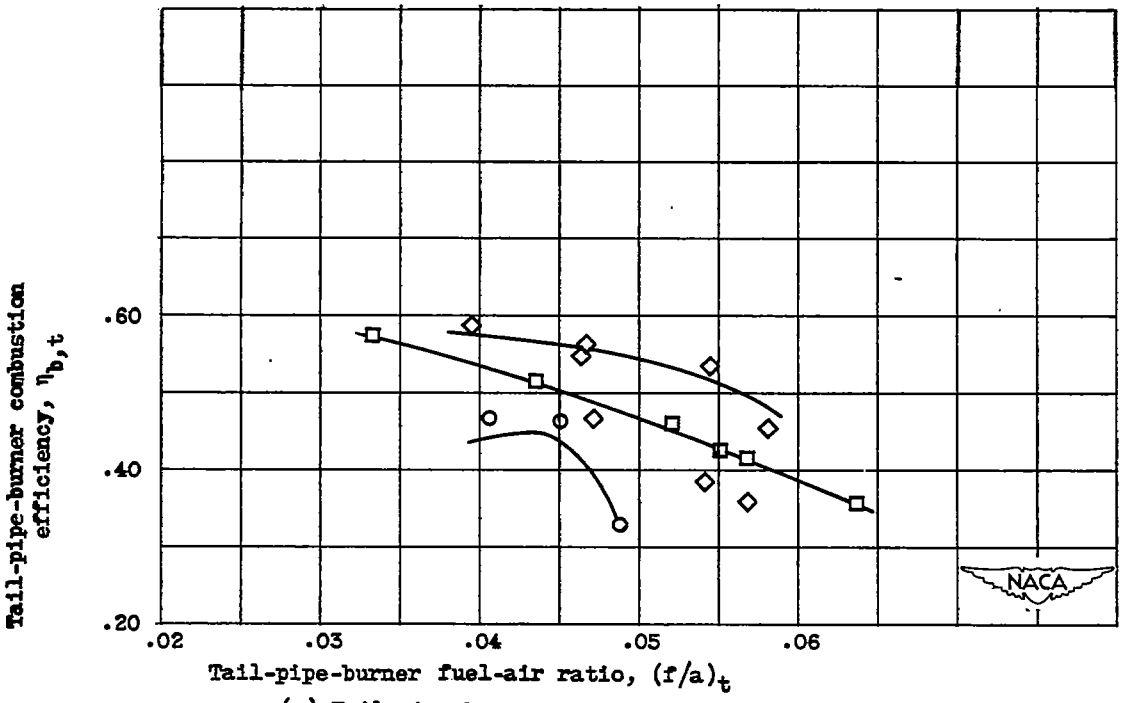

(e) Tail-pipe-burner combustion efficiency.

Figure 12. - Concluded. Variation of performance with tail-pipe fuel-air ratio for configurations A, B, and C. Altitude, 35,000 feet; flight Mach number, 0.21; engine speed, 7900 rpm; engine-inlet total temperature, 500° R ± 10°.

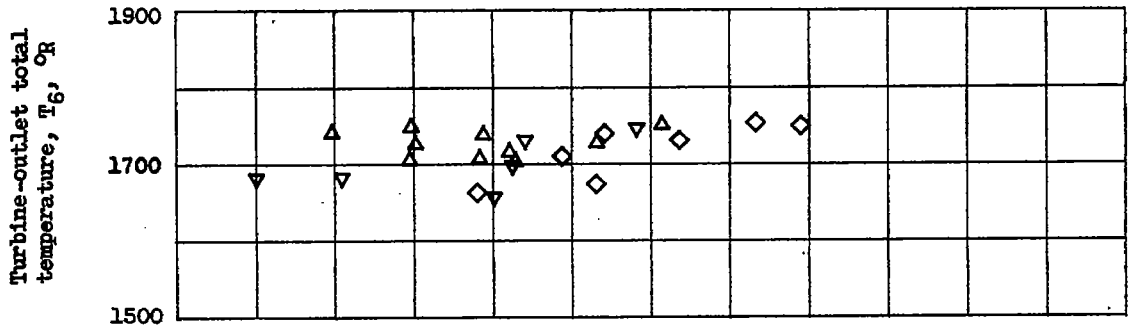

(a) Turbine-outlet total temperature.

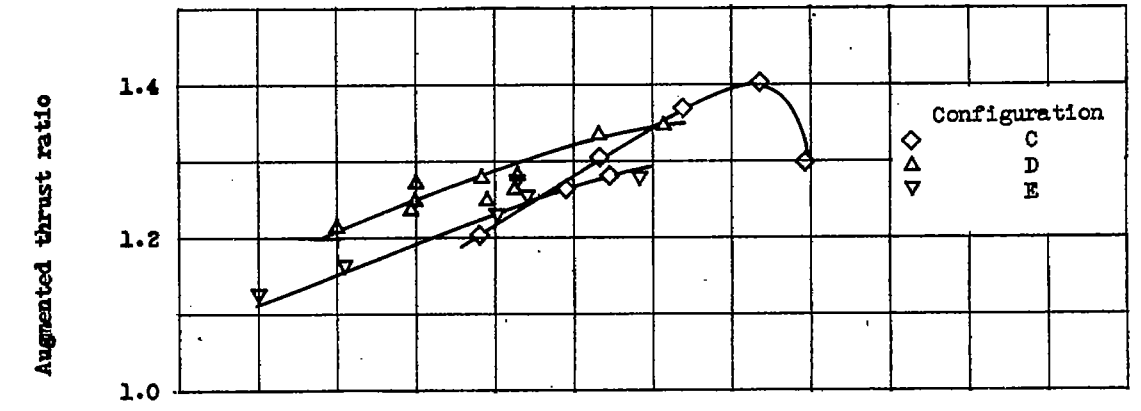

(b) Augmented thrust ratio.

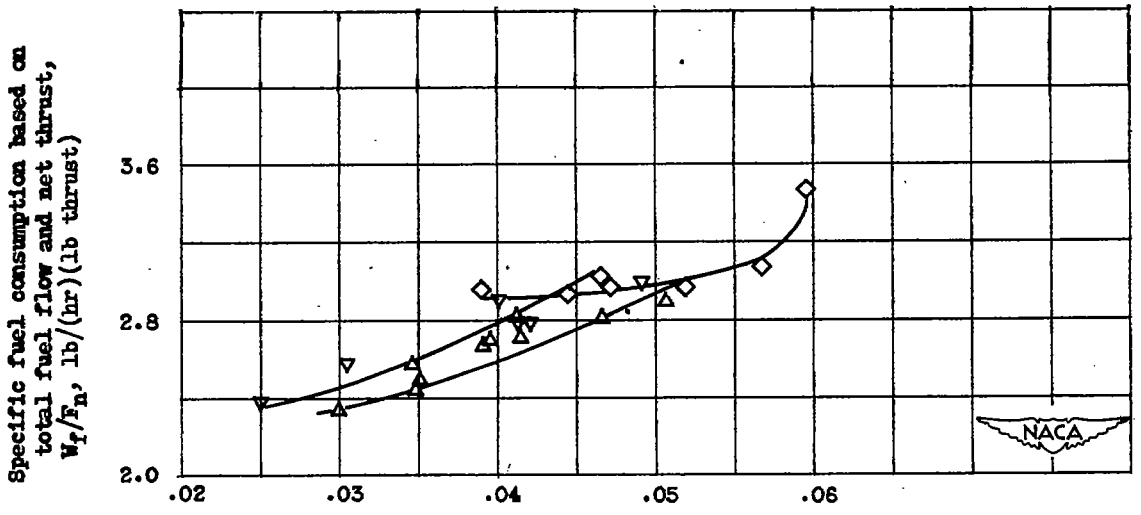

(c) Specific fuel consumption.

Figure 13. - Variation of performance with tail-pipe fuel-air ratio for configurations C, D, and E. Altitude, 25,000 feet; flight Mach number, 0.21; engine speed, 7900 rpm; engine-inlet total temperature, 500° R ± 10°.

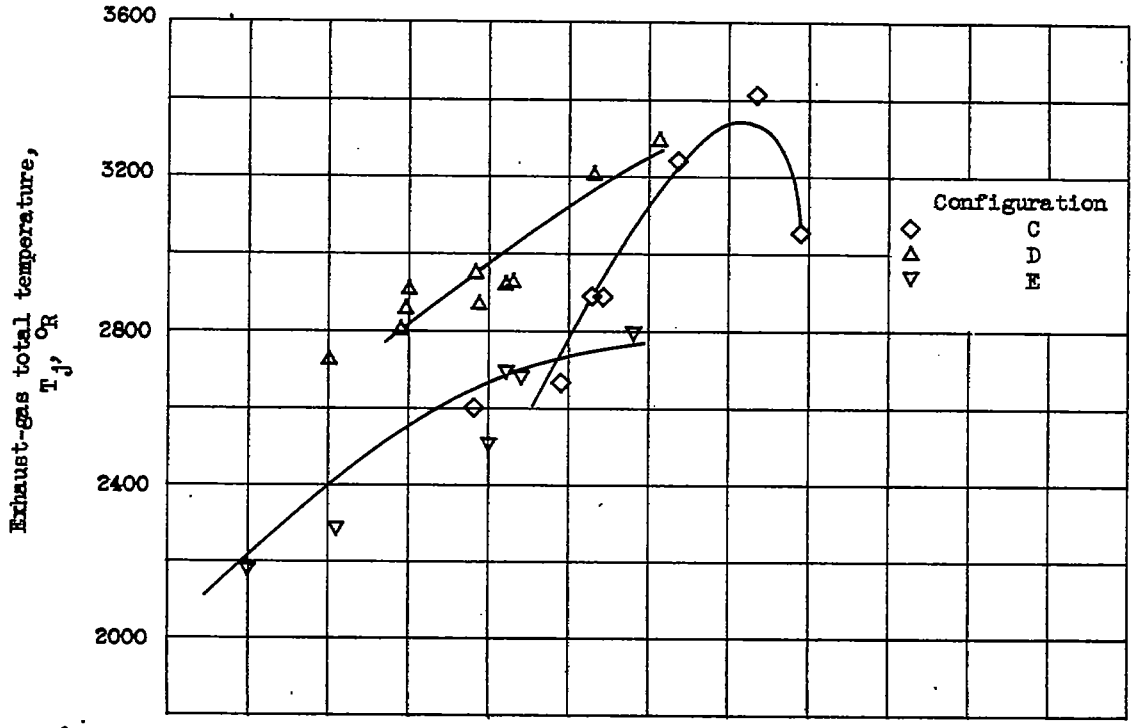

(d) Exhaust-gas total temperature.

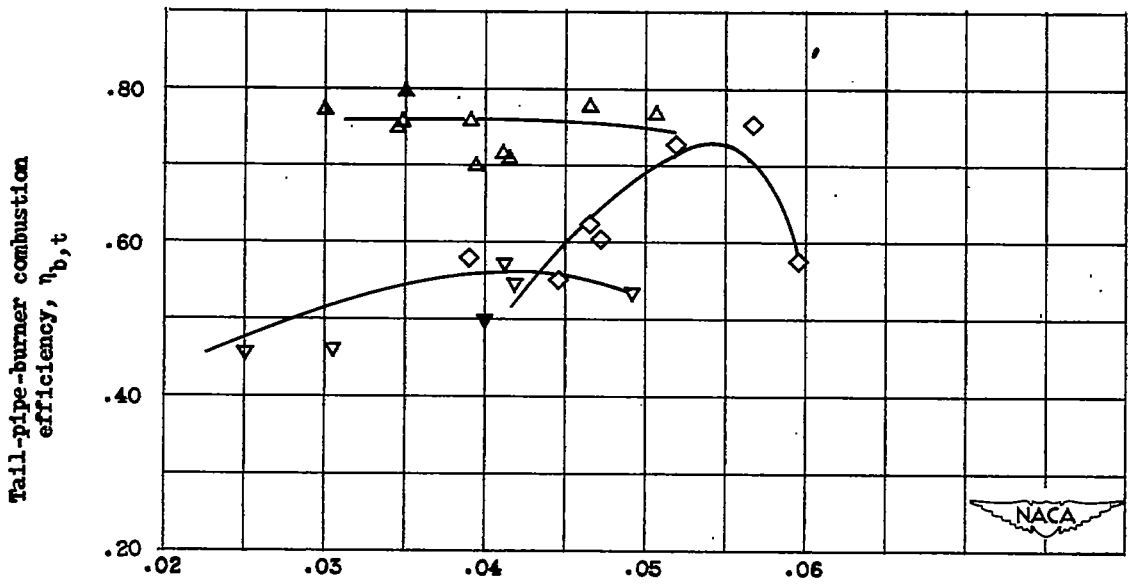

Tail-pipe-burner fuel-air ratio, $(f/a)_t$

(e) Tail-pipe burner combustion efficiency.

Figure 13. - Concluded. Variation of performance with tail-pipe fuel-air ratio for configurations C, D, and E. Altitude, 25,000 feet; flight Mach number, 0.21; engine speed, 7900 rpm; engine-inlet total temperature, 500° R ± 10°.

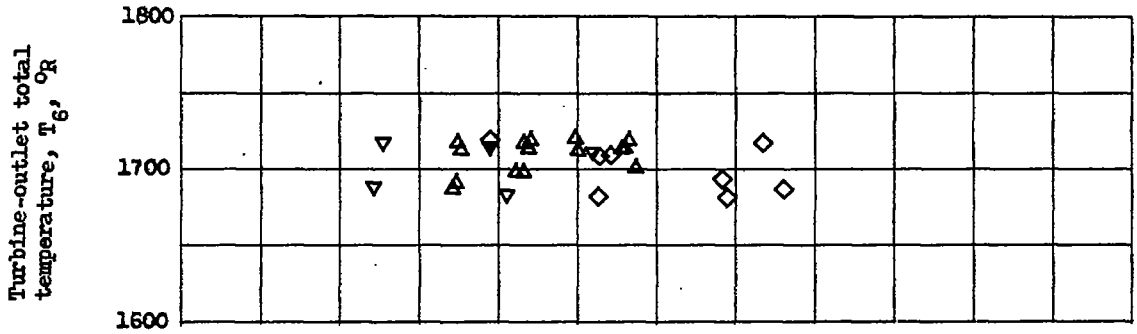

(a) Turbine-outlet total temperature.

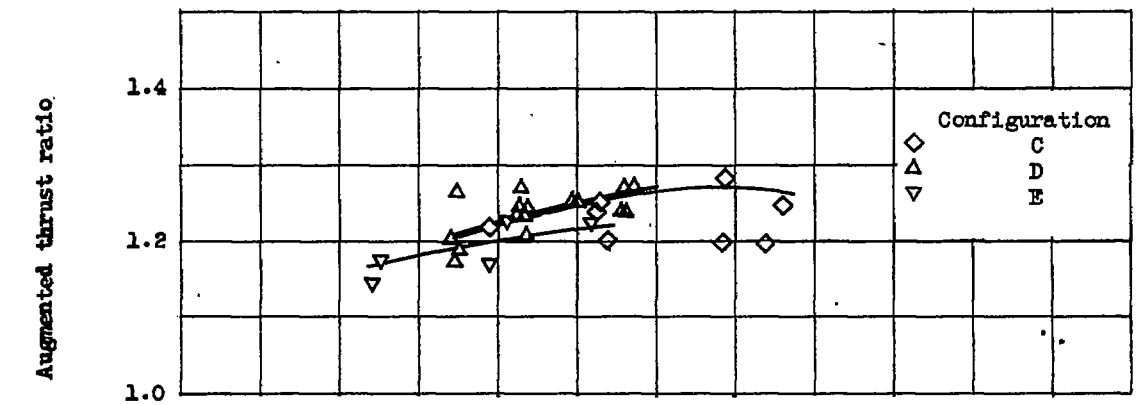

(b) Augmented thrust ratio.

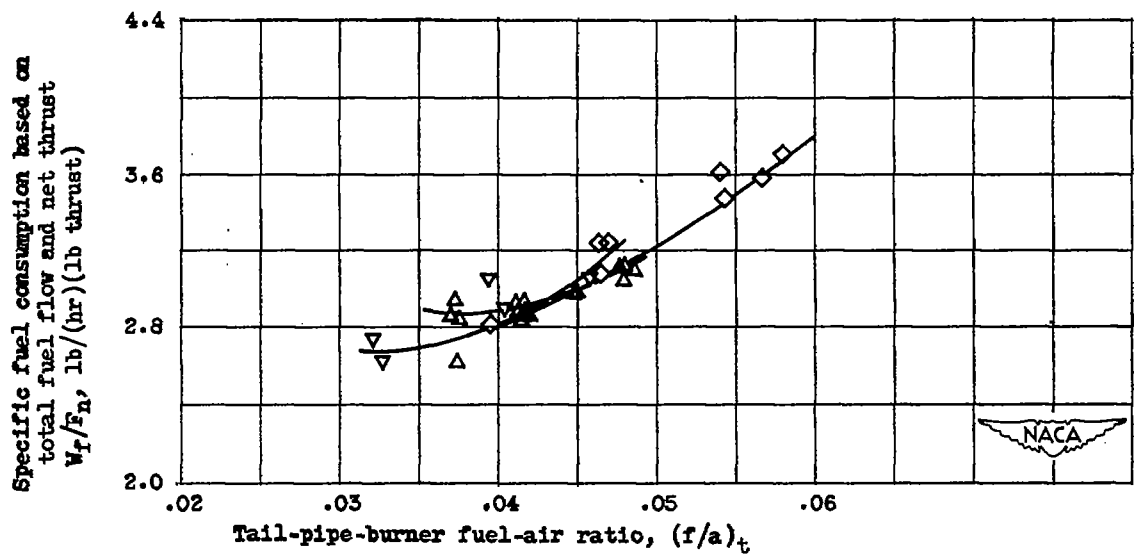

(c) Specific fuel consumption.

Figure 14. - Variation of performance with tail-pipe fuel-air ratio for configurations C, D, and E. Altitude, 35,000 feet; flight Mach number, 0.21; engine speed, 7900 rpm; engine-inlet total temperature, 500° R ± 10°.

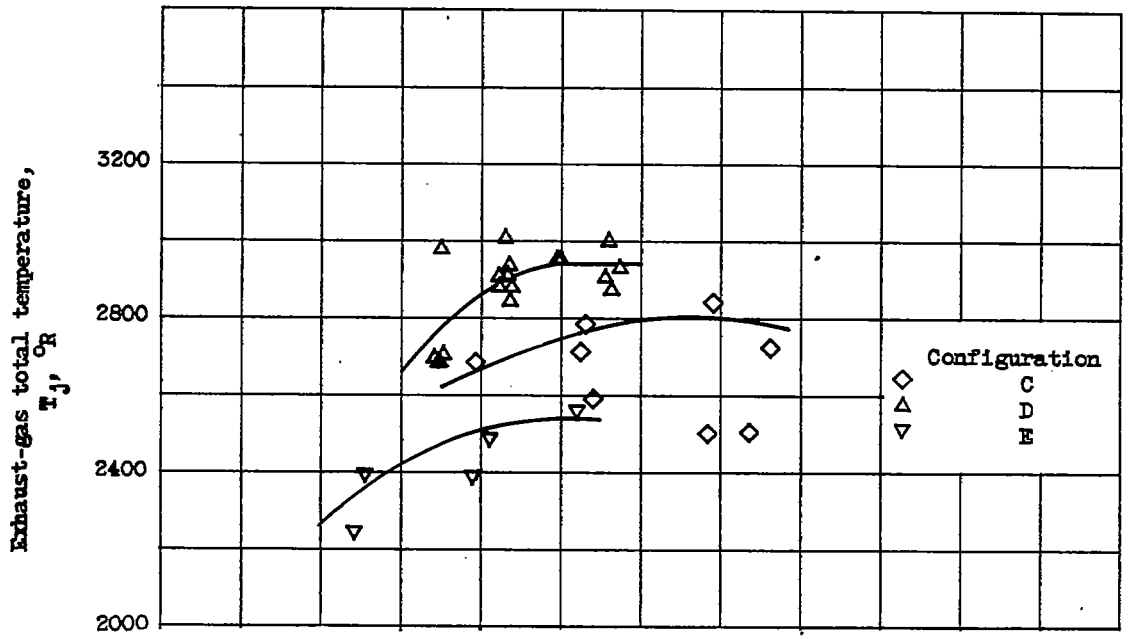

(d) Exhaust-gas total temperature.

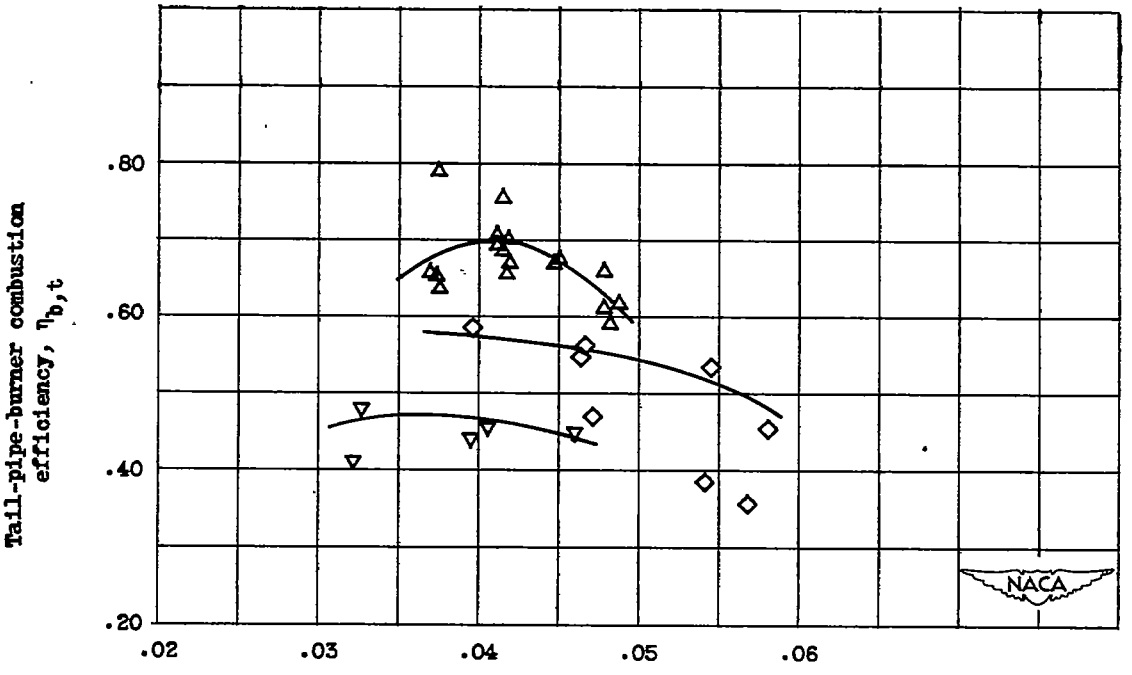

(e) Tail-pipe-burner combustion efficiency.

Figure 14. - Concluded. Variation of performance with tail-pipe fuel-air ratio for configurations C, D, and E. Altitude, 35,000 feet; flight Mach number, 0.21; engine speed, 7900 rpm; engine-inlet total temperature, 500° R ± 10°.

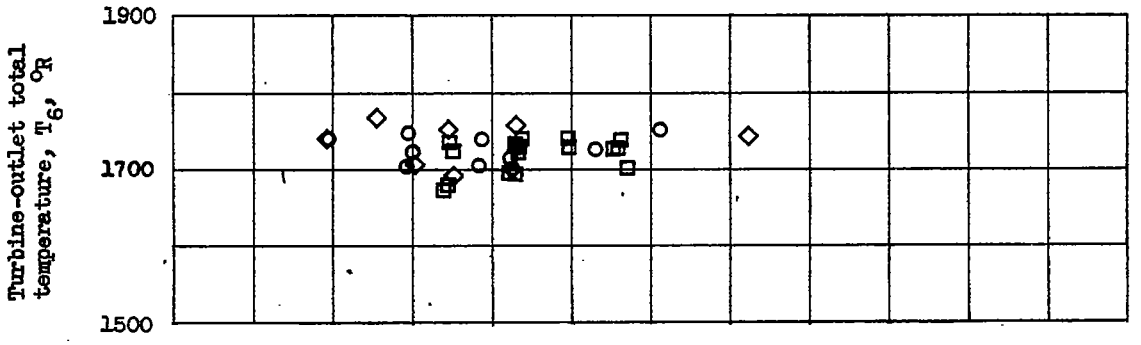

(a) Turbine-outlet total temperature.

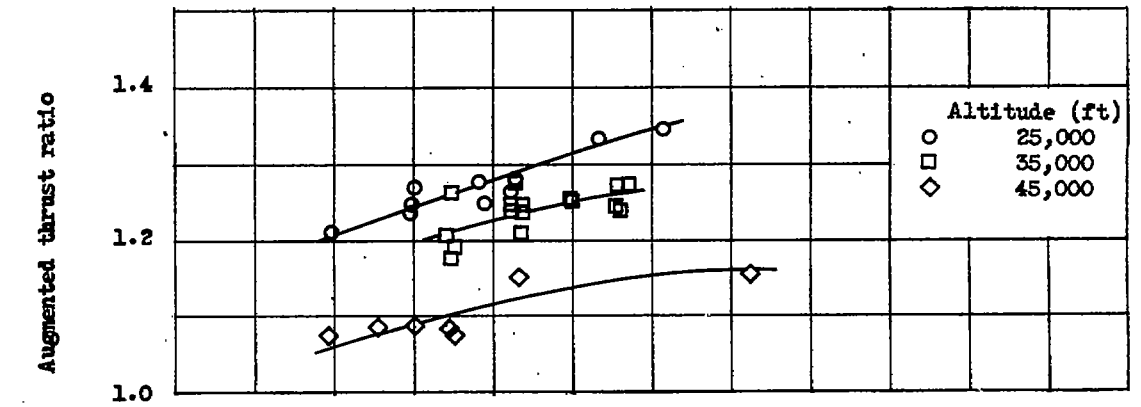

(b) Augmented thrust ratio.

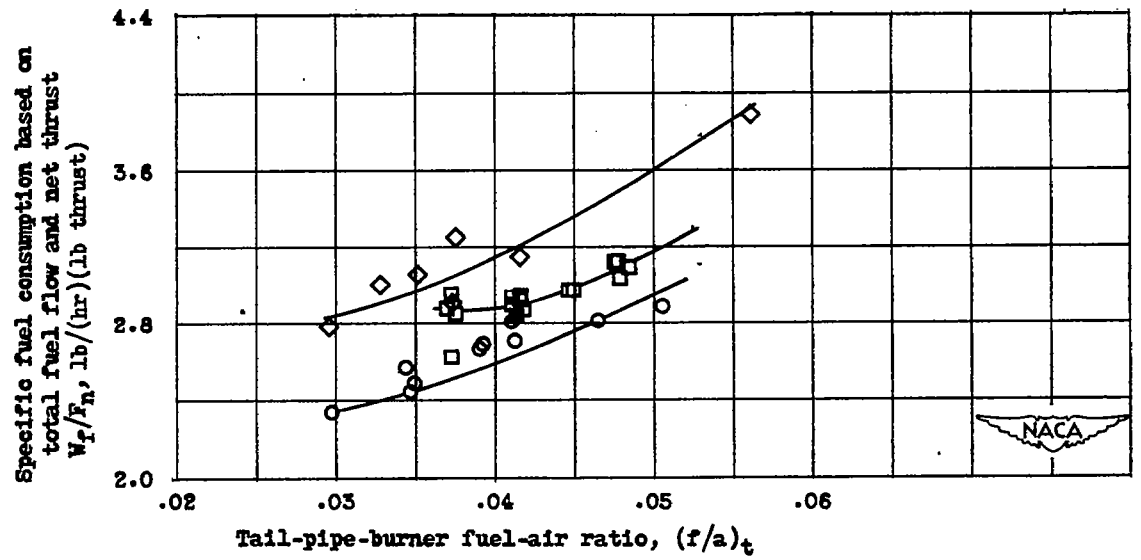

(c) Specific fuel consumption.

Figure 15. - Effect of altitude on variation of performance with tail-pipe fuel-air ratio for configuration D. Flight Mach number, 0.21; engine speed, 7900 rpm; engine-inlet total temperature, 500° R ± 10°.

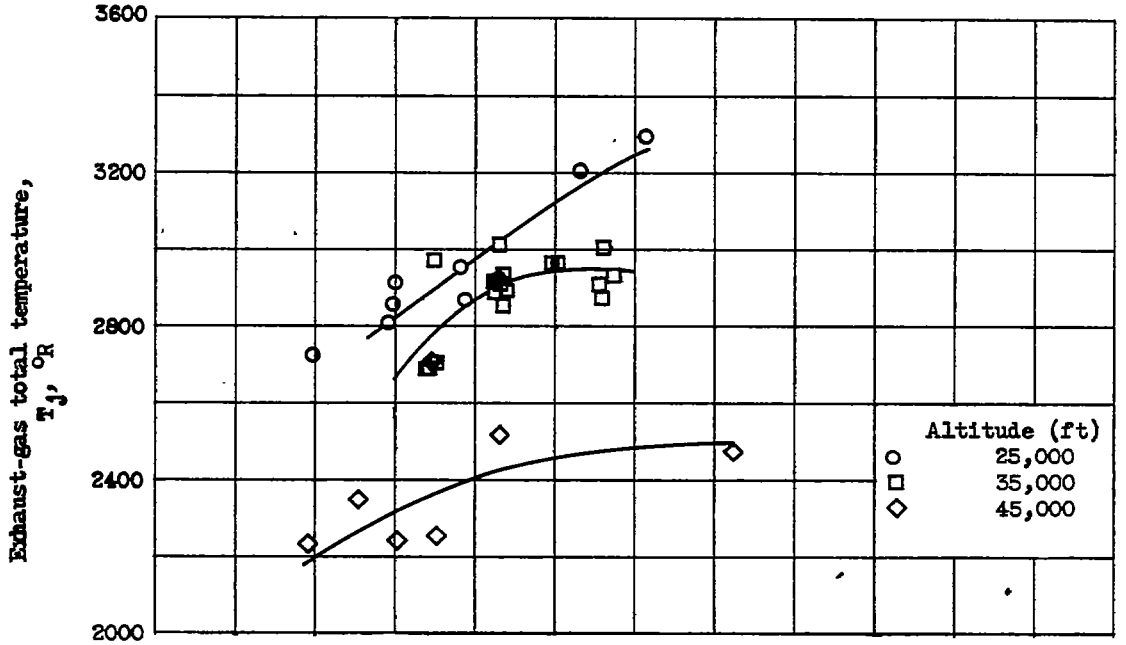

(d) Exhaust-gas total temperature.

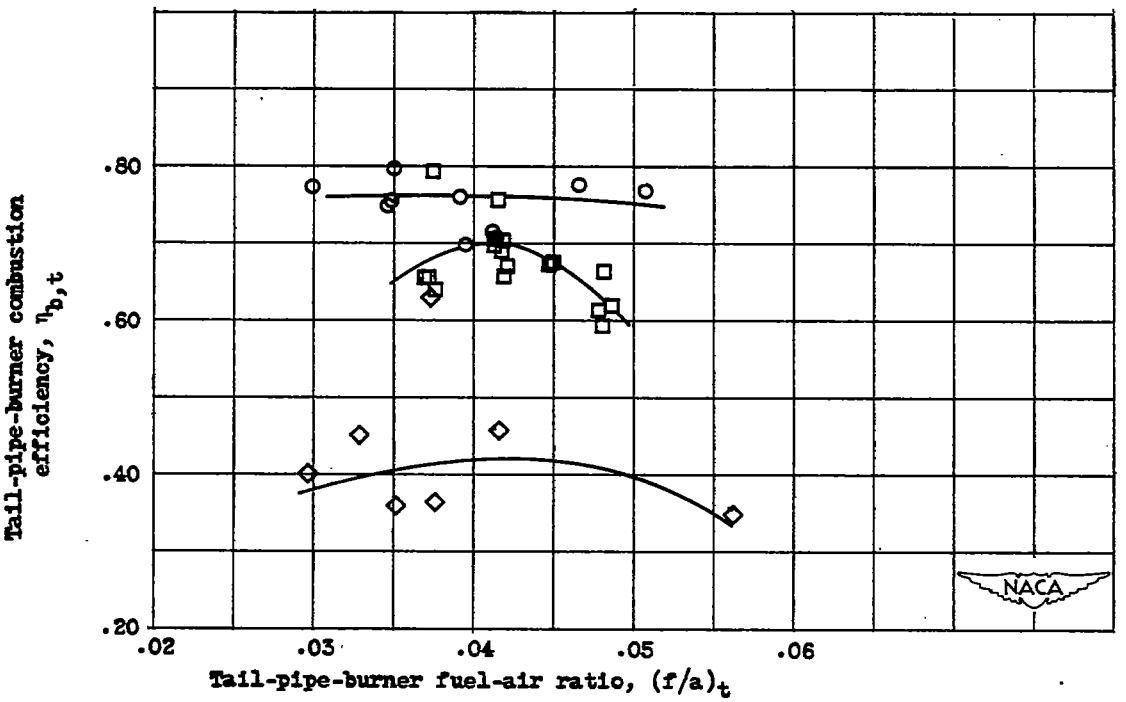

(e) Tail-pipe-burner combustion efficiency.

Figure 15. - Concluded. Effect of altitude on variation of performance with tail-pipe fuel-air ratio for configuration D. Flight Mach number, 0.21; engine speed, 7900 rpm; engine-inlet total temperature, 500° R ± 10°.

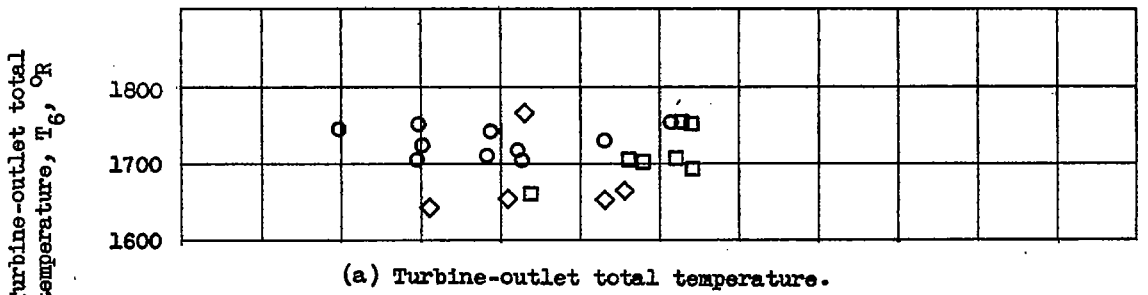

(a) Turbine-outlet total temperature.

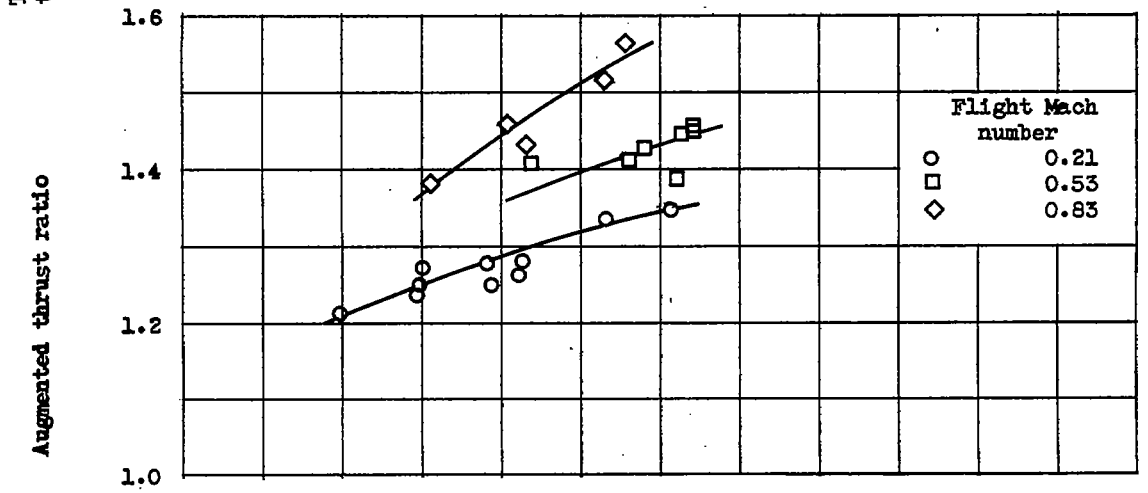

(b) Augmented thrust ratio.

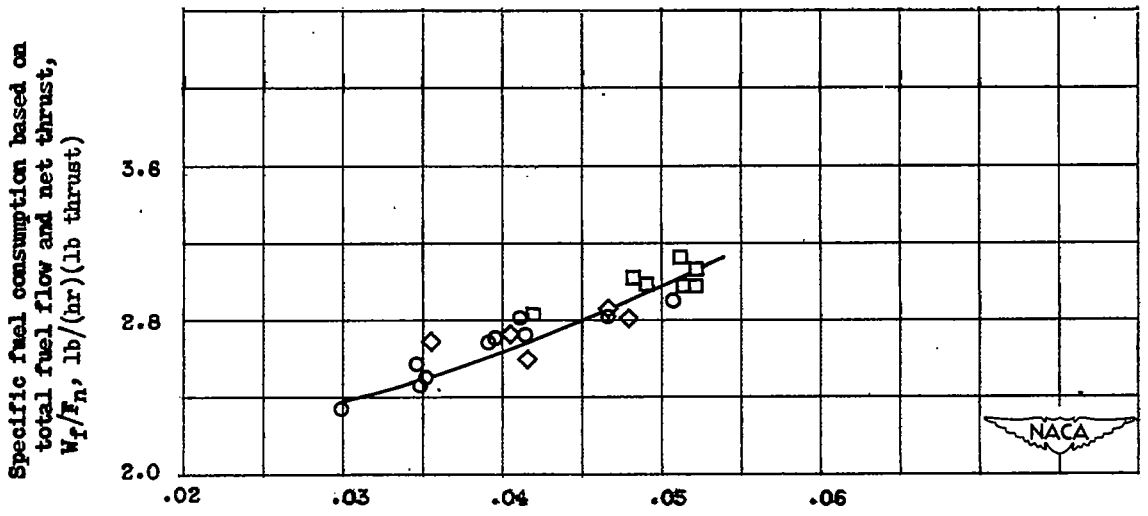

(c) Specific fuel consumption.

Figure 16. - Effect of flight Mach number on variation of performance with tail-pipe fuel-air ratio for configuration D. Altitude, 25,000 feet; engine speed, 7900 rpm; engine-inlet total temperature, 500° R ± 10°.

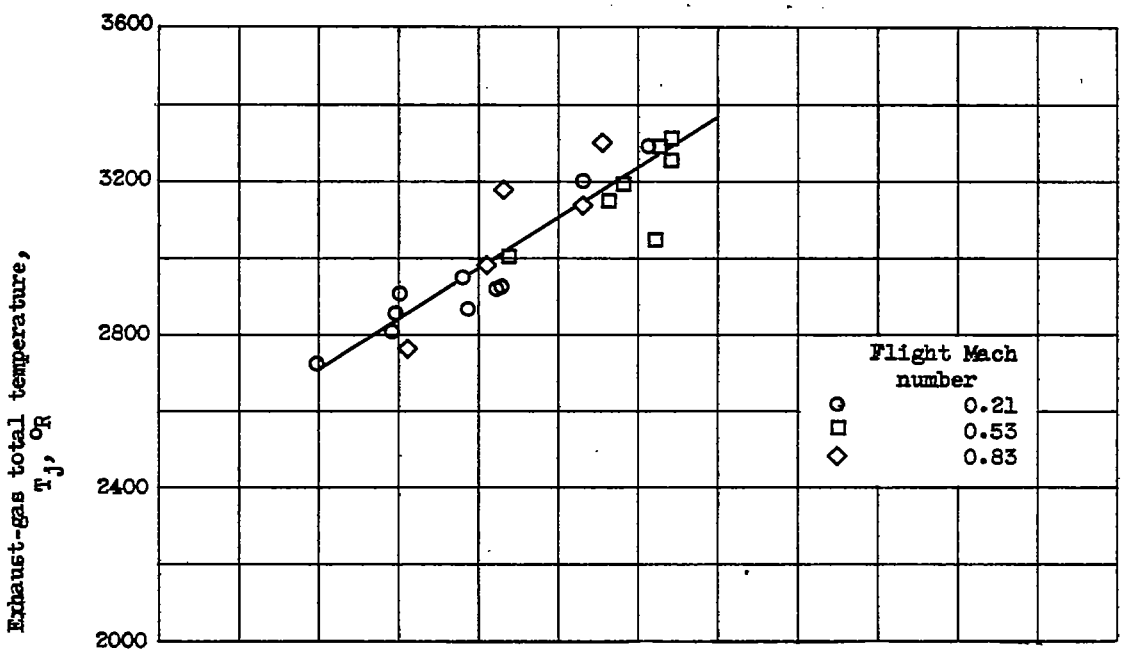

(d) Exhaust-gas total temperature.

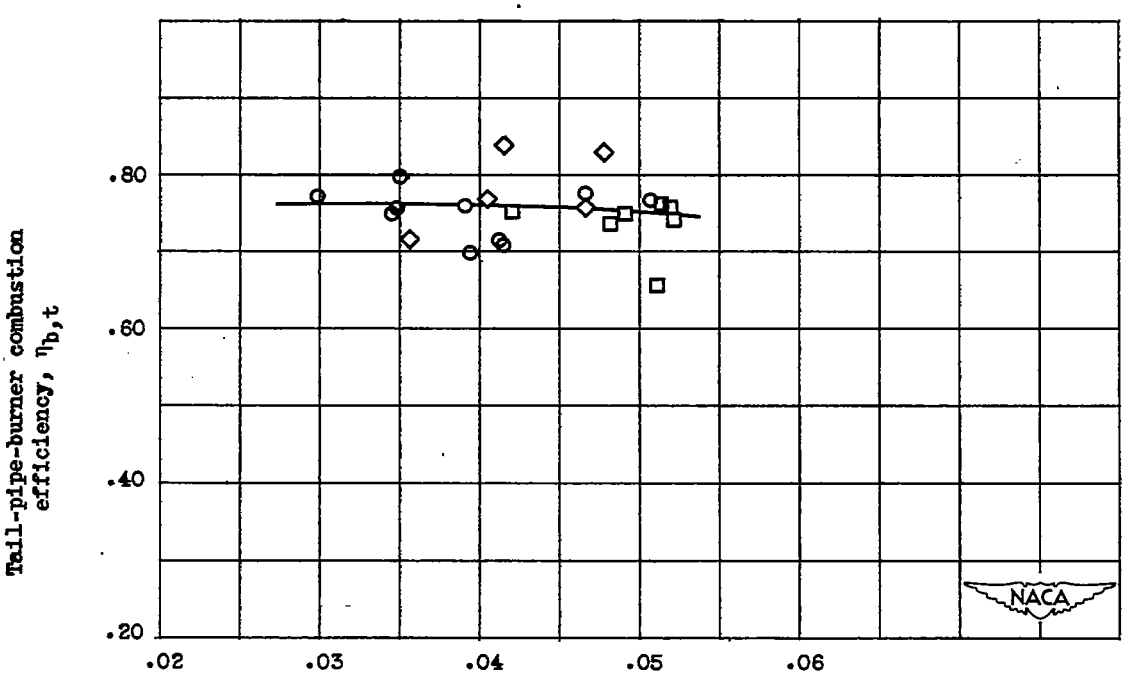

(e) Tail-pipe-burner combustion efficiency.

Figure 16. - Concluded. Effect of flight Mach number on variation of performance with tail-pipe fuel-air ratio ratio for configuration D. Altitude, 25,000 feet; engine speed, 7900 rpm; engine-inlet total temperature, 500° R ± 10°.

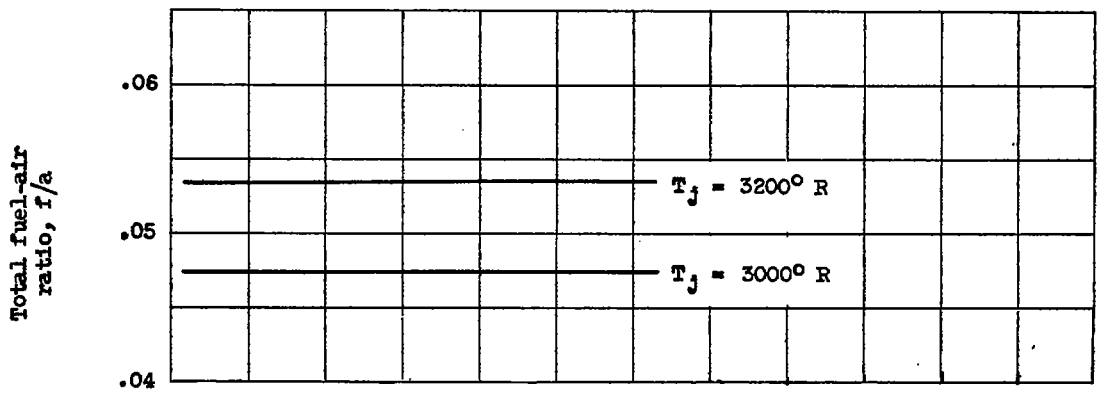

(a) Total fuel-air ratio.

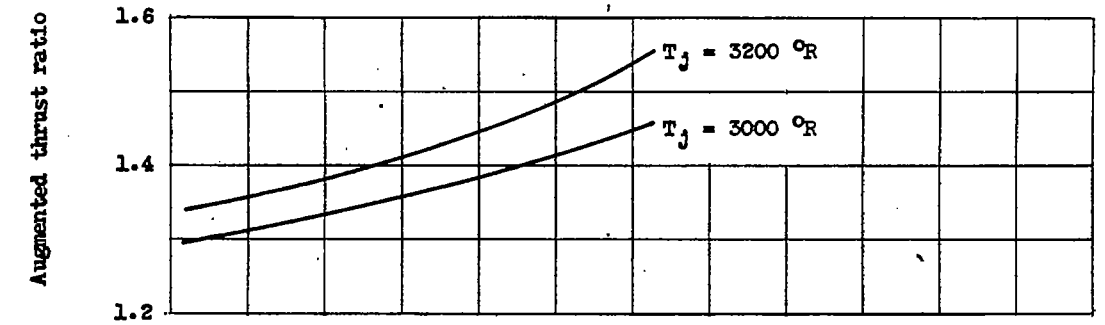

(b) Augmented thrust ratio.

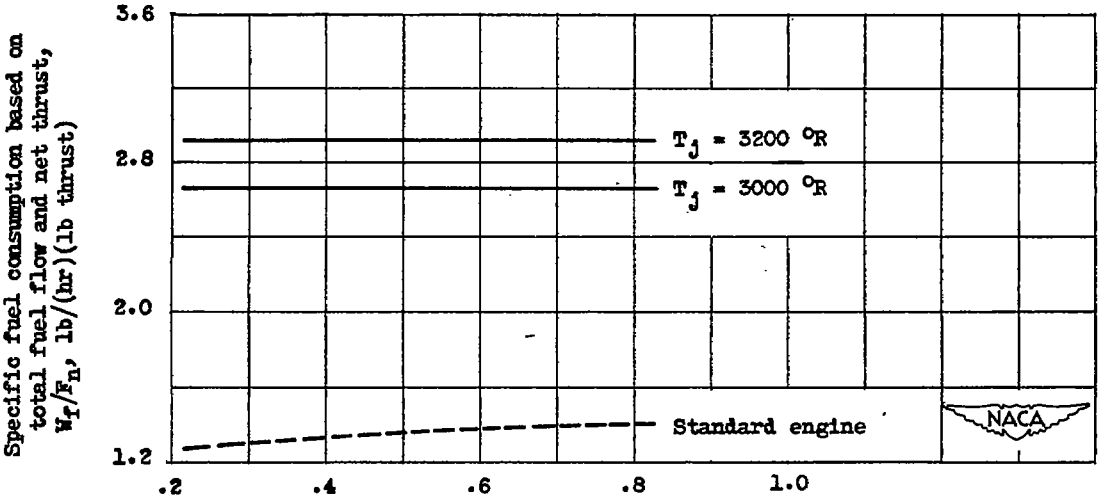

(c) Specific fuel consumption.

Figure 17. - Variation of total fuel-air ratio, augmented thrust ratio, and specific fuel consumption with flight Mach number for two exhaust-gas total temperatures (for configuration D). Altitude, 25,000 feet; engine speed, 7900 rpm; average turbine-outlet total temperature, 1710° R; engine-inlet total temperature, 500° R ± 10°.

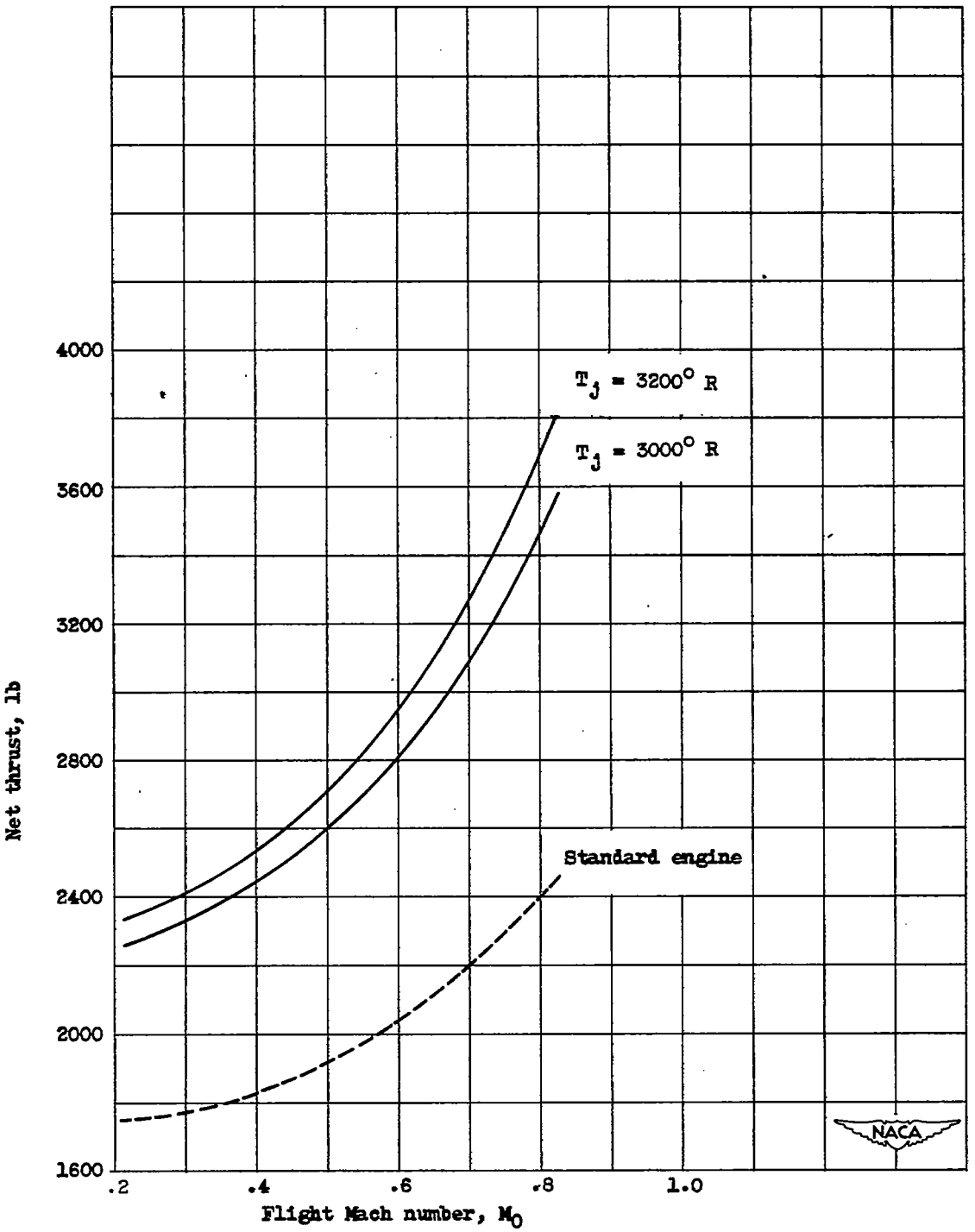

Figure 18. - Variation of net thrust with flight Mach number for two exhaust-gas total temperatures (for configuration D). Altitude, 25,000 feet; engine speed, 7900 rpm; average turbine-outlet total temperature, 1710° R; engine-inlet total temperature, 500° R ± 10°

[redacted]

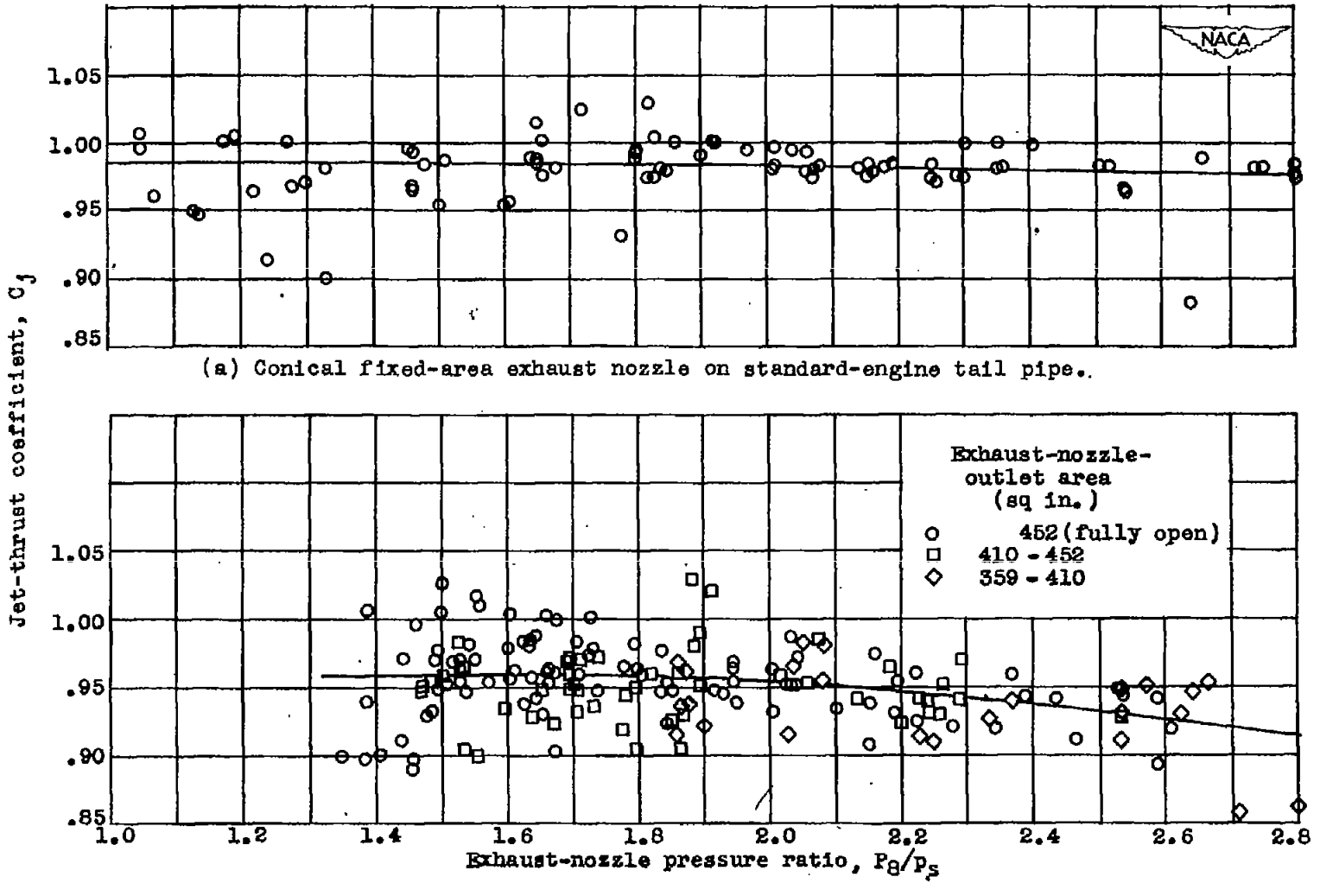

(a) Conical fixed-area exhaust nozzle on standard-engine tail pipe.

(b) Variable-area exhaust nozzle on tail-pipe burner.

Figure 19. - Variation of jet-thrust coefficient with exhaust-nozzle pressure ratio.